ANL-6152
Particle Accelerators and
High-Voltage Machines
(TID-4500, 15th Ed.)
AEC Research and
Development Report

ARGONNE NATIONAL LABORATORY
9700 South Cass Avenue
Argonne, Illinois

PARTICLE ACCELERATOR DIVISION

Summary Report

May 1959 through March 1960

Albert V. Crewe,	Director
John P. FitzPatrick,	Associate Director
Martyn H. Foss,	Associate Director
David S. Manson,	Assistant Director

Previous Summary Reports:

ANL-5630	April 1956 through September 1956
ANL-5713	October 1956 through March 1957
ANL-5803	April 1957 through September 1957
ANL-5864	October 1957 through April 1958
ANL-5956	April 15, 1958 through October 1958
ANL-6032	November, 1958 through May 1959

Operated by The University of Chicago
under
Contract W-31-109-eng-38

DISCLAIMER

TABLE OF CONTENTS

PARTICLE ACCELERATOR DIVISION

Summary Report

I. PUBLICATIONS

Abstracts of ANLAD Reports

ANLAD-57 "Radial Motions in the 50-Mev Linear Accelerator"
David Cohen (July 16, 1959)

Radial orbit motions have been computed with the IBM-704 for the Argonne 50-Mev injector linac. By direct examination of particular orbits the effects of the following phenomena were investigated: translational, rotational, and gradient misalignments of the quadrupole magnets; nonlinear forces due to transit-time factor variations with radius, and also the presence of the magnet ends; the complete loss of excitation power to one or more magnets. By means of acceptance and emittance figures in phase space, an investigation was made of the effects of these phenomena: variation of the radiofrequency phase at injection into the linac; opening of the bore down the linac; ripple from the quadrupole magnet power supplies; space charge of the proton beam. Orbits and phase-space figures are presented, usually in both the ++-- and +-+- modes of magnet rotations. Tolerances are deduced from the misalignment studies, the nonlinear effects are shown to be negligible, and the loss of one magnet is shown generally to be serious. Radiofrequency effects can be seen to be significant only at low magnet gradients in the ++-- mode. Ripple tolerances are discussed and variations of several percent are found to be allowable. Space-charge studies indicate that more than 50 milliamperes must be injected into the linac before the effects become noticeable.

ANLAD-58 "Analytical Studies of the $2\nu_y - \nu_x = 1$ Resonance"
Lee C. Teng (November 10, 1959)

The computing machine programs written for the study of the $2\nu_y - \nu_x = 1 (\nu_x = \frac{3}{4}, \nu_y = \frac{7}{8})$ resonance indicate so far that within the ranges of values of the parameters for the ZGS and the errors assumed, the coupling effect of this resonance is too small to be seen in tens of revolutions. This result, while being reassuring, leaves an unsatisfactory feeling. One would certainly want to know just exactly how small is the coupling effect. To continue running the program to hundreds or thousands of revolutions is futile, because of the growing accumulated errors in computation and financial limitations. An approximate analytical solution giving the effect of this resonance is attempted here. The approximate results do, indeed, support the computing machine findings that for the ZGS this resonance is completely unimportant.

ANLAD-59 "Transverse Space Charge Effects"
Lee C. Teng (February 1, 1960)

The conventional calculation of transverse space-charge defocusing effect in circular magnetic accelerators for circular beam cross section is improved and extended to take into account the realistic elliptical shape of the beam cross section. This results in an entirely different trajectory of migration of the operating point (ν_x, ν_y) due to space-charge effect and, hence, a different set of limiting resonance lines. The result indicates that the space-charge limit of the beam intensity in the ZGS is approximately between 4×10^{13} and 7×10^{13} protons/pulse, depending on which resonance line is fatal and the distribution of protons along the equilibrium orbit at injection. Several effects tending to reduce the space-charge limit are discussed. Close examination shows also that compensation of the space-charge defocusing effect by varying the focusing action of the guide magnetic field is impractical. On the other hand, it is likely that by artificially injecting free electrons into the vacuum chamber total neutralization of the transverse space-charge defocusing effect can be achieved. This is studied.

Internal Memoranda

E. H. Berkowitz

EHB-1 — Suggestions Concerning Flash Bouncer System for the 300-kv Cockcroft-Walton (October 22, 1959)

Robert Borchers

*RB-PVL-1 — Performance Characteristics of the Vacion Pump (November 12, 1959)

G. O. Calabrese

GOC-15 — Arc-back Expectancies with 144 and 192 Rectifiers for the ZGS Power Supply (January 27, 1960)

E. A. Crosbie

EAC-4 — Some Comments Concerning the Design of the DC Magnets (July 27, 1959)

---

* Indicates joint authorship

G. D. Doolen

GDD-1	An Investigation of the Inductance and Capacitance in the Control Cable to Determine Effects on Relays in the Cable Circuit (June 17, 1959)
GDD-2	Thermistor Flow Switch (September 18, 1959)

R. George

RG-2	A Stored Interpretive Routine Enabling Neology (March 14, 1960)

H. A. Kampf

HAK-8	Controlling Back Resistances Variation for Series Connected Diodes (July 2, 1959)
HAK-9	Power Supply Using Silicon Diodes (July 10, 1959)

W. Leonchick

*WL-THM-1	Ring Vacuum System (November 13, 1959)

P. V. Livdahl

*RB-PVL-1	Performance Characteristics of the Vacion Pump (November 12, 1959)

T. H. McGreer

THMcG-3	A New Approach to the Control of the Power Supply Generator at Injection (August 11, 1959)
*WL-THM-1	Ring Vacuum System (November 13, 1959)

J. Moenich

JSM-6	"Spacemetal" Chamber (March 30, 1960)

W. A. Siljander

WAS-5	Ring Magnet Coil Design - Part II (July 31, 1959)

---

* Indicates joint authorship

W. F. Stevens

WFS-1	An Introduction to Computers and Their Use (September 11, 1959)

A. A. Strassenburg

AAS-4	The Attenuation and Propagation Constants for a Wave Guide of Finite Conductivity (September 9, 1959)

M. Striegl

*AY-MS-1	A Preliminary Calculation on Trajectories of Non-paraxial Rays (October 29, 1959)

L. C. Teng

LCT-11	Fringing Field at a Simple Two-dimensional Magnet Edge (June 15, 1959)
LCT-12	Isochronous Variable-Energy Multi-Particle Cyclotron (June 30, 1959)
LCT-14	Design Parameters for the DC Magnets of the ZGS (August 12, 1959)
LCT-15	Asymmetric Achromatic Bending Magnet System (November 5, 1959)
LCT-16	Phase Space and Beam Qualities (March 3, 1960)
LCT-17	Lagrangian Formulation of the Motion of a Charged Particle in an Electromagnetic Field (March 7, 1960)
LCT-18	Solutions of Systems of Linear Equations with Slowly Varying Coefficients (March 30, 1960)

R. Trcka

*RT-WDZ-2	Brookhaven National Laboratory Foundation Summary (May 1, 1959)
*RT-WDZ-3	Summary of Soil and Geological Conditions at ANL (June 17, 1959)

---

* Indicates joint authorship

K. Weberg

KW-2	Characteristics of Grounding Systems (July 13, 1959)

A. Yokosawa

*AY-MS-1	A Preliminary Calculation on Trajectories of Non-paraxial Rays (October 29, 1959)
AY-1	Some Plasma Physics Involved with the Ion Source (January 11, 1960)
AY-2	An Ion Source Which Produces a Hydrogen Ion Current of 1,000 MA (February 12, 1960)
AY-3	I. Extraction System for an RF Ion Source (March 23, 1960)

W. D. Zander

*RT-WDZ-2	Brookhaven National Laboratory Foundation Summary (May 1, 1959)
*RT-WDZ-3	Summary of Soil and Geological Conditions at ANL (June 17, 1959)

External Publications

Elastic Proton-Deuteron Scattering at 450 Mev
A. V. Crewe, B. Ledley, E. Lillethun, S. Marcowitz, L. G. Pondrom
The Physical Review, 114, 1361-1365 (1959).

Notes on External Particle Beams from the Argonne 12.5 Bev Synchrotron
A. V. Crewe
Proceedings of the International Conference on High-Energy Accelerators and Instrumentation, September 14-19, 1959.

The Argonne Zero Gradient Synchrotron (ZGS)
A. V. Crewe
Proceedings of the International Conference on High-Energy Accelerators and Instrumentation, September 14-19, 1959.

---

* Indicates joint authorship

Charge Independence in the Reactions $p + d \longrightarrow \pi^0 + He^3$ and $p + d \longrightarrow \pi^+ + H^3$ at 450 Mev
A. V. Crewe, S. Marcowitz, B. Ledley, E. Lillethun, C. Rey
The Physical Review (in press)

Standard Pulse Generator
R. E. Daniels, C. Swoboda
Electronics
Submitted February, 1960

Acceleration of Polarized Protons with Strong-Focusing Linear Accelerators
David Cohen, Alan J. Burger
The Review of Scientific Instruments, 30, 1134-1135 (1959).

II. RING MAGNET POWER SUPPLY

A. Status Report - E. F. Frisby

The specification for the ring magnet power supply was completed on July 10, 1959, and three companies: Westinghouse, General Electric and Allis-Chalmers, submitted proposals for furnishing this equipment on September 25, 1959. Several months were required for evaluating the material contained in the proposals and executing the procurement contract. A preaward meeting was held with each of the prospective vendors during the evaluation period for the purpose of giving the various companies an opportunity to clarify and supplement the information contained in their individual proposals. The contract was awarded to the Allis-Chalmers Manufacturing Company on February 5, 1960.

The motor-generator set for the power supply as proposed by the successful bidder will consist of two 3-phase generators rated at 34,620 rms kva each, a wound rotor motor rated at 14,500 hp, and a 68-ton flywheel interposed between the two generators. The total weight of the motor-generator set has been estimated to be 841,000 pounds. The generators will be connected to four rectifier transformers rated at about 17,000 kva each. Figure 1 indicates the component interconnection scheme in single line form. The primary connections on the transformer will be delta-wye, and the secondary connections will be 6-phase double-wye. The details of this connection scheme are shown in Figure 2. A total of 144 pumped tubes of the Excitron type will be used in the main rectifying units. The rectifiers will be connected in a parallel-series scheme similar to that in the Bevatron. There will be four parallel-series rectifier banks connected to the magnet coil terminals - one bank at each of the four supply points around the magnet. Using this connection scheme, it has been calculated that the voltage to ground at the magnet terminals will be of the order of 1,350 volts. The terminal-to-terminal voltage at each supply point will be approximately 2,700 volts. The total series voltage around the magnet coils has been calculated to be approximately 10,700 volts when operating at full power. According to calculations, the maximum current will be about 11,000 amperes at peak power.

Other features of the power supply include the utilization of a liquid rheostat for controlling the power swing on the power lines and to control speed during operation. Dynamic braking will be used for slowing down the motor-generator set when normal operation is suspended. The generator exciter will furnish the power for dynamic braking. Auxiliary equipment, which includes shorting switches, grounding equipment and arc-gaps, is being purchased with the ring magnet power supply for the protection of the ring magnet coil.

According to the delivery schedule, some of the power supply components should start arriving at the Laboratory during February, 1961,

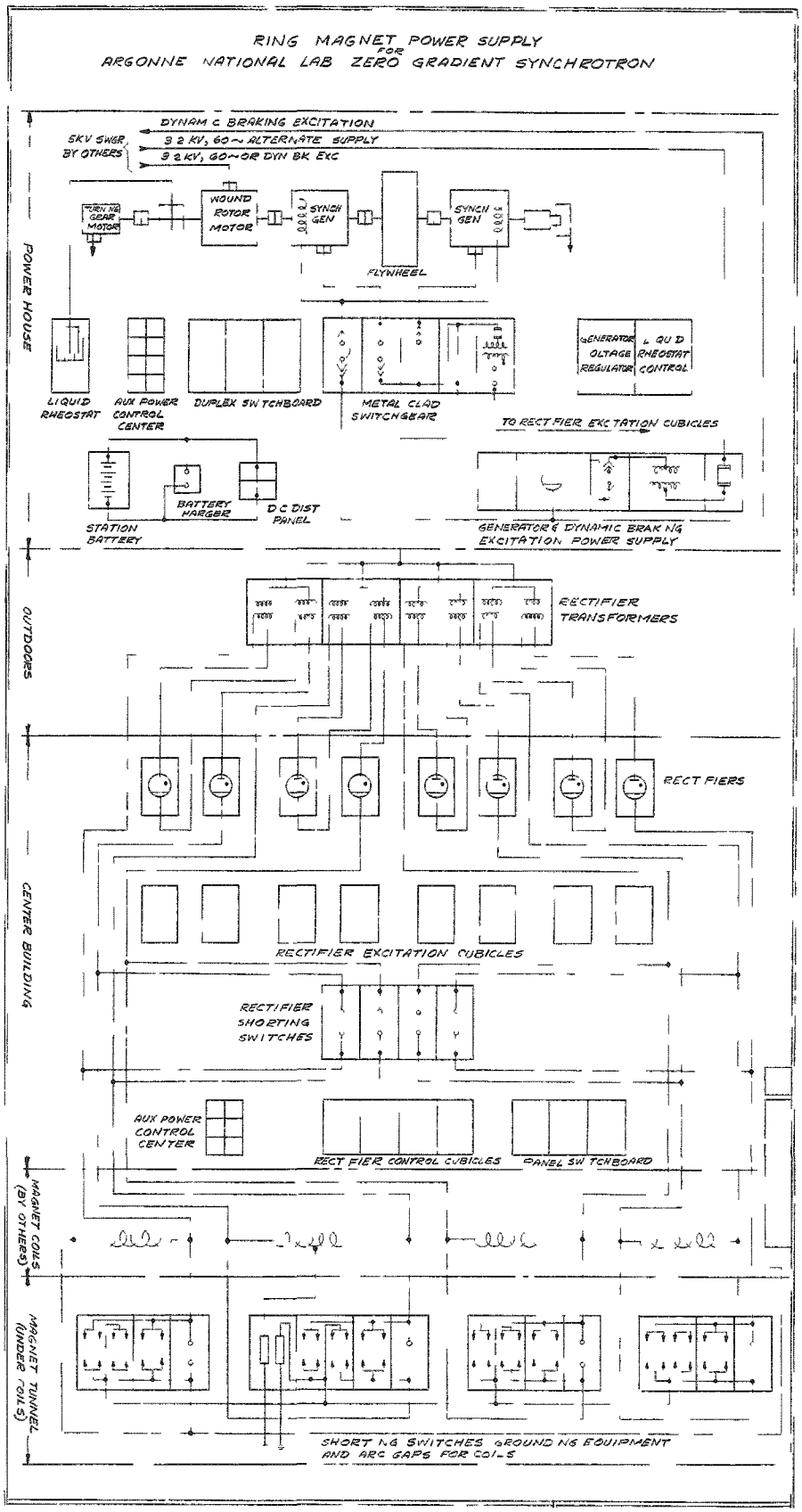

Fig. 1

Magnet Power Supply for ANL ZGS - Block and Single Line Diagram

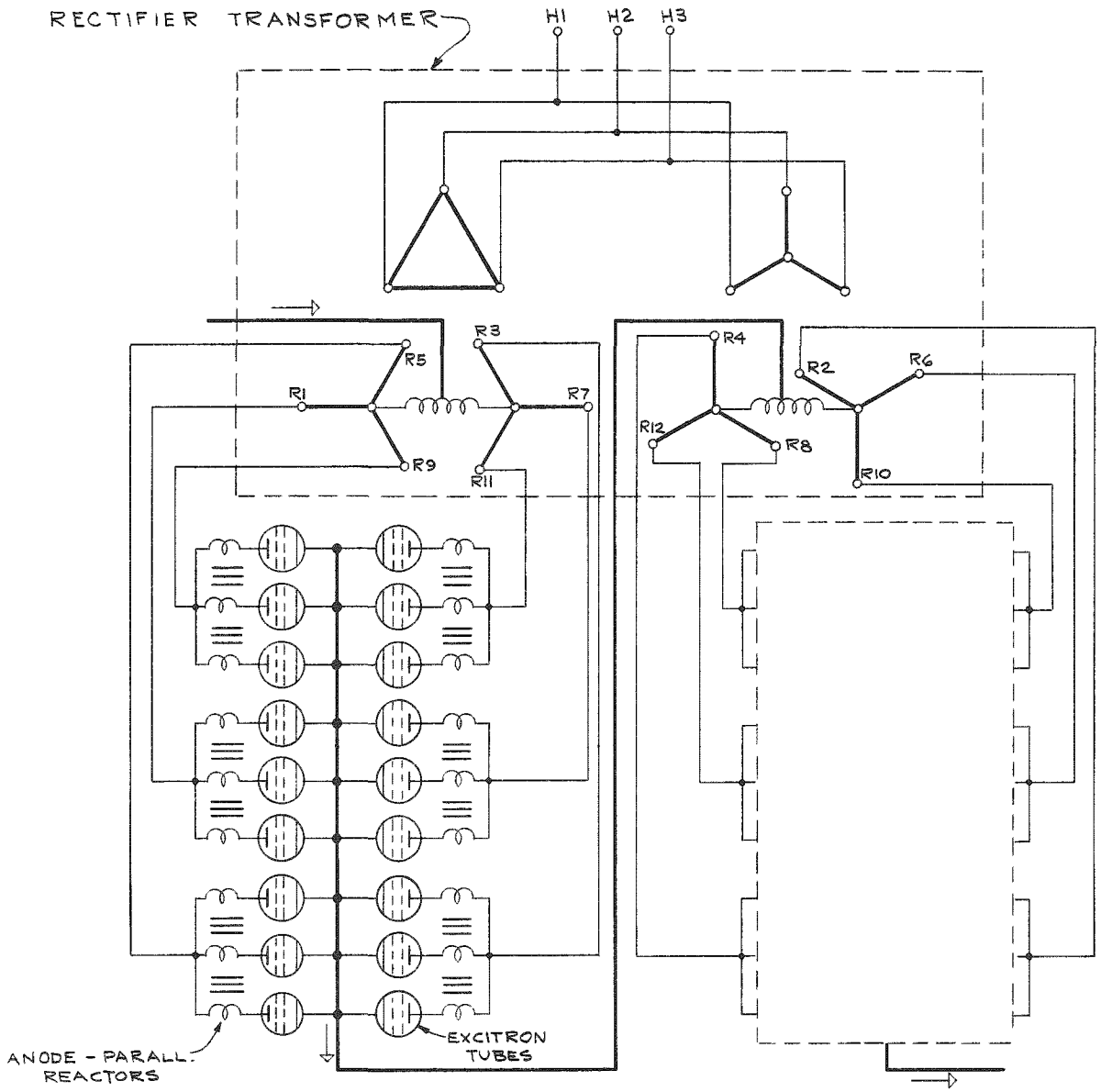

Fig. 2

Connection Diagram of Rectifier Transformer and
Two 18-tube Rectifiers Connected in Cascade

and final shipment should be made in May, 1961. It is anticipated that the equipment will be installed and ready for field testing in approximately eight months after delivery.

B. Effect of the Magnet Voltage Regulation Method on the Power Requirements, the Radiofrequency Accelerating Voltage and the Number of Accelerating Gaps - G. O. Calabrese (Calculations made by R. Pawula)

These effects were studied for five possible cases or methods of operation of the magnet voltage as follows:

Case I — The voltage e_1 across the magnet varies linearly from the initial value at the rate of 30% per second

Case II — As in Case I except that the rate of clearance is 25% per second

Case III — The voltage e_1 remains constant during the whole rising period

Case IV — The flux density during the rising period increases at a constant rate of 22.5 kgauss/sec

Case V — The magnet current i during the rising period increases linearly at the rate of 10,950 amp/sec

The results of this study are summarized in the Summary Table on page 13.

The total accelerating voltage V_a which it is necessary to produce across the radio frequency accelerating gap is obtained from the values of $\frac{dB}{dt}$ from this table by means of the expression

$$V_a = \frac{3.862}{h} \frac{dB}{dt} \quad ,$$

where h is the number of gaps.

Considerations of radiofrequency power requirements have led to the decision on the part of the RF Group to make h = 3.

C. Harmonics of Power Supply - G. O. Calabrese (Calculations made by R. Pawula)

Table I shows the results of the calculations of the amplitudes of the harmonic currents and voltages obtained at the end of the rising period and during flat topping with the parallel and with the cascade connections. The values of the angle α shown at the top of the table are the values of the phase angle control required to obtain the magnet voltages required during flat topping.

SUMMARY TABLE

(Different Magnet Voltage Regulation Modes)

Case	$\frac{di}{dt}$, $\frac{amp}{sec}$		e_1, kv			$\frac{dB}{dt}$, $\frac{kgauss}{sec}$		rms Current, amp [1]	Maximum Inst. Power, Mw	Equip. Rating,[2]		Eddy Current, ampere turns	
	Initial	Final	Initial	Max.	Final	Initial	Final			Mw	%	Initial	Final
I (e_1 = 12.2-3.66t) kv	11,736	27,864	12.2	12.2	8.47	30.01	13.57	5054	92.645	61.66	100	2514	1136
II e_1 = (12.2-3.05t) kv	11,724	31,974	12.2	12.2	9.222	30.01	15.42	4415	100.953	59.96	97.24	2514	1290
III e_1 = 10.6 kv	10,197	39,001	10.6	10.6	10.6	26.08	18.80	4827	116.049	51.17	82.99	2142	1574
IV $\frac{dB}{dt}$ = 22.5 kgauss	8,782	45,667	9.133	12.089	12.089	22.5	22.5	4709	132.374	56.93	92.33	1884	1884
V $\frac{di}{dt}$ = 10.95 kamp/sec	10,950	10,950	11.388	12.778	5.146	28.05	5.40	5096	78.761	65.12	105.61	2350	652

[1] Over the 4-sec pulsing period

[2] Referred to magnet terminals, that is max dc voltage at terminals of magnet by I_{rms}.

Table I

AMPLITUDES OF HARMONICS UNDER DIFFERENT CONDITIONS

(Including the effect of commutation and assuming a 25% voltage drop from no load to full load)

Harmonic	Frequency (cps)	Amplitudes of Harmonics at the End of the Rising Period			Amplitudes of Harmonics during Flat Topping								
					Parallel			Cascade			Cascade		
		Parallel and Cascade			$\alpha = 60.5°$, $u = 29.9°$			Bank on Invert / Bank on Rectify			All Banks on Rectify		
		$\alpha = 0°$ $u = 60°$						$\alpha = 90.9°$, $u = 30.1°$ / $\alpha = 0°$, $u = 60°$			$\alpha = 60.5°$, $u = 29.9°$		
A	B	(volts) C	i (amp) D*	B (gauss) D_1^*	(volts) E	i (amp) F*	B (gauss) F_1^*	(volts) G	i (amp) H*	B (gauss) H_1^*	(volts) I	i (amp) J*	B (gauss) J_1^*
6	360	0	0	0	0	0	0	276.1	2.44	5.014	0	0	0
12	720	223.8	0.989	2.032	479.6	2.12	4.356	346.9	1.53	3.144	479.6	2.12	4.356
18	1080	0	0	0	0	0	0	87.6	0.258	0.530	0	0	0
24	1440	110.5	0.244	0.501	238.4	0.527	1.083	162.7	0.360	0.740	238.4	0.527	1.083
30	1800	0	0	0	0	0	0	54.0	0.096	0.197	0	0	0
36	2160	73.4	0.108	0.222	158.8	0.234	0.481	98.6	0.145	0.298	158.8	0.234	0.481
42	2520	0	0	0	0	0	0	39.5	0.050	0.103	0	0	0
48	2880	55.1	0.061	0.125	118.8	0.131	0.269	64.2	0.071	0.146	118.8	0.131	0.269
54	3240	0	0	0	0	0	0	30.9	0.030	0.062	0	0	0
60	3600	44.0	0.039	0.080	95.2	0.084	0.173	41.1	0.036	0.074	95.2	0.084	0.173
66	3960	0	0	0	0	0	0	24.6	0.020	0.041	0	0	0
72	4320	36.7	0.027	0.055	73.6	0.054	0.111	14.8	0.011	0.023	73.6	0.054	0.111
78	4680	0	0	0	0	0	0	19.5	0.013	0.027	0	0	0
84	5040	31.4	0.020	0.041	67.8	0.043	0.088	18.2	0.011	0.023	67.8	0.043	0.088
90	5400	0	0	0	0	0	0	14.9	0.0088	0.018	0	0	0
96	5760	27.5	0.015	0.031	59.3	0.033	0.068	14.8	0.0082	0.017	59.3	0.033	0.068
102	6120	0	0	0	0	0	0	10.6	0.0055	0.011	0	0	0
108	6480	24.4	0.012	0.025	52.7	0.026	0.053	15.7	0.0077	0.016	52.7	0.026	0.053

*Disregarding the effect of the corresponding eddy currents in the iron.

Regarding the cascade connection, the figures of columns G and H are based on the assumption that two banks are left on rectify at $\alpha = 0$ as at the end of the rising period and two banks are shifted to $\alpha = 90.9°$. This combination may not necessarily represent the best combination of α values for minimizing the amplitudes of the harmonics that will prove troublesome. The figures in the I and J columns represent the amplitudes of the harmonics obtained with $\alpha = 60.5°$ on all four banks, this value of α being the value that must be used with the parallel connection in order to obtain the required magnet voltage. Evidently the figures of columns I and J coincide with those of columns E and F.

From the amplitudes of the harmonic currents in columns D, F, H and J, we have calculated the amplitudes of the individual harmonic flux densities shown in columns D_1, F_1, H_1, J_1.

D. Correlation of Synchrotron Oscillation Frequencies to Harmonic Flux Densities - G. O. Calabrese (Calculations made by A. Burger)

For Cases IV and V of the modes of voltage regulation at the magnet terminals we have calculated the synchrotron oscillation frequencies f_s by means of the following expression supplied by L. Teng

$$f_s = \frac{2.67}{\gamma} \frac{dB}{dt} \left(\frac{1}{a} - \frac{1}{\gamma^2} \right) ,$$

where

$$a = 0.554$$

$\frac{dB}{dt}$ is expressed in kgauss/sec

and

$$\gamma = \sqrt{1 + 0.48145\ B^2} .$$

Here B is expressed in kgauss.

The results are plotted in Figure 3.

For Case IV, Table II shows the harmonic frequencies which approximately fall near the synchrotron frequencies at specified times during the rising period. No attempt has been made to match exactly the harmonics and the synchrotron frequencies because the speed vs time variation and the exact values of the harmonic frequencies are not available.

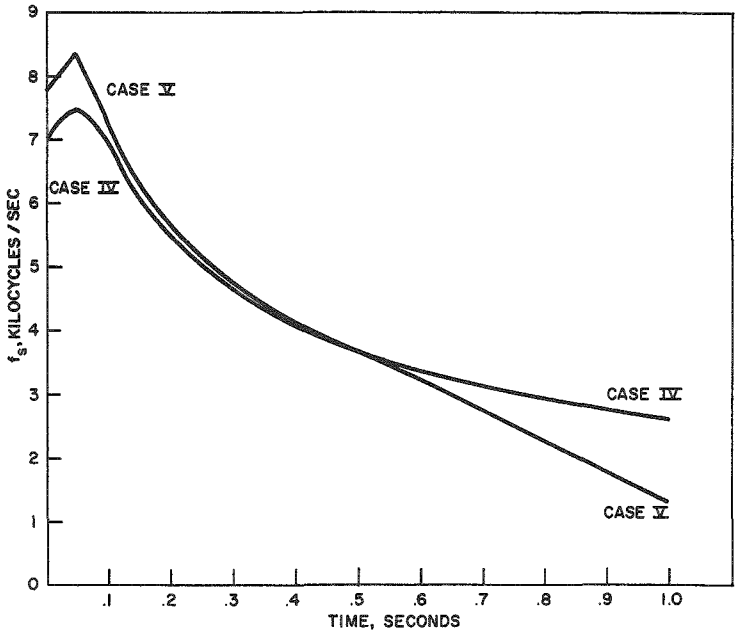

Fig. 3

Synchrotron Oscillation Frequencies

E. Effect of Duration Δt of Flat Topping on the Motor and Flywheel Requirements for the ZGS under Different Conditions - G. O. Calabrese (Calculations made by A. Burger and R. Pawula)

Assuming an overall efficiency of 90% for the combination generator-transformer-rectifier, the motor average output M_0 for three different flat topping durations Δt is as shown below.

Δt (sec)	M_0 (Mw)	hp
0	7.81	10470
0.1	8.75	11729
0.2	9.68	12976

These values represent the smallest possible size of motor.

For $\Delta t = 0.2$ sec, assuming a motor of 9.68 Mw, the total flywheel requirements, $W'R^2$, for synchronous speeds of 3600, 900 and 720 rpm and 4 different values of the slip s_1 at the end of the flat topping period are shown in Table III.

Figure 4 shows the speed change and the instantaneous power flow to and from various components during one pulse assuming a constant motor input.

Table II

CORRELATION OF SYNCHROTRON OSCILLATION FREQUENCY TO HARMONIC VOLTAGES, CURRENT AND FLUX DENSITIES

t, sec	f_s,[1] kcps	Harmonic[2] with Same Frequency	n[3]	Current,[4] amperes	u, Degree[5]	A_n,[6] volts	B_n,[6] volts	V,[7] volts	i_n,[8] amp	B_n,[9] gauss
0	6.954	120	10	0	0	0	-0.423672	0.423672	0.000037	0.000095
0.10	7.004	120	10	875	16.3	-6.59587	-2.92608	7.21577	0.00063	0.0016
0.20	5.601	96	8	1750	23.1	6.41909	-11.0124	12.7466	0.0014	0.0036
0.30	4.691	84	7	2625	28.3	-13.4752	10.2718	16.9437	0.0022	0.0056
0.40	4.112	72	6	3500	32.8	-21.1424	8.31647	22.7192	0.0034	0.0087
0.50	3.695	60	5	4375	36.8	19.8638	-23.9222	31.0940	0.0052	0.013
0.60	3.382	60	5	5250	40.5	-16.9713	41.1282	44.4922	0.0080	0.020
0.70	3.253	48	4	6175	44.1	32.8788	28.2473	43.3465	0.0086	0.022
0.80	3.136	48	4	7175	47.7	-30.6370	-36.9600	48.0069	0.012	0.030
0.90	3.032	48	4	8500	52.3	49.6961	6.26059	30.0889	0.018	0.043
1.00	2.937	48	4	10950	60.0	55.0149	-1.98577	55.0507	0.060	0.125

[1] Based on Case IV.

[2] Rounded to the nearest multiple of 12.

[3] n is the harmonic order.

[4] Based on Case IV.

[5] $\cos u = 1 - I_c X_c \Big/ \left(\sqrt{2E_s \sin\frac{\pi}{3}}\right)$, where $2E_s = 3686$ and $X_c = 0.583\Omega$ (based on Case II) and $I_c = \frac{1}{4}$ of total current (u = commutation angle).

[6] Assuming $\alpha = 0$, this holds both for parallel and cascade connection.

[7] $V = \sqrt{A_n^2 + B_n^2}$

[8] $i_n = \dfrac{V}{2\pi f \frac{L_s}{4}}$

[9] $B_n = \dfrac{B_T}{I_T} i_n$

Table III

FLAT TOPPING PERIOD

Δt^1 = 0.2 sec
(M_0 = 9.68 Mw)

Frequency of supply, cycles/sec	60	60	60
Number of poles of induction motor	2	8	10
Synchronous speed n_s (rpm)	3600	900	720
Assumed slip at t_0, s_0 (%)	1	1	1
Speed at t_0, n_0 (rpm)	3564	891	713
n_0^2	12.702×10^6	0.79388×10^6	0.50837×10^6
Total energy supplied by flywheel in the interval (0.1012, 1.2), 10^6 joules	54.726	54.726	54.726

K_1*	Slip s_1[2] at $t_1 + \Delta t$ = 1.2 sec	$W'R^2$ (10^6 lb ft^2)		
0.90	10.9	0.0982	1.571	2.453
0.92	8.92	0.1222	1.956	3.054
0.94	6.94	0.1602	2.564	4.004
0.96	4.96	0.2379	3.806	5.944

*$K_1 = n_1/n_0$ where n_1 = speed at the end of the rising period

[1]For $\Delta t = 0$ and the same speed slips (s_1)

M_0 = 7.81 Mw and the total energy to be supplied by the flywheel is 50.900×10^6 joules so that the ($W'R^2$) required will be 0.9301 times the values shown above.

[2]$s_1 = 1 - (1 - s_0) K_1 = 1 - 0.99 K_1$.

F. Arc-back Expectancies with 144 and 192 Rectifiers for the ZGS Power Supply - G. O. Calabrese

In order to determine whether we should purchase 48 rectifiers in addition to the 144 contemplated by the power supply contract with the Allis-Chalmers Company, we have made calculations of the arc-back expectancies with and without the additional rectifiers for Cases III and IV.

The actual calculations were performed on computer 704 F by the Applied Mathematics Division with data supplied by us. A summary of the results is given in Table IV.

The expectancies shown in this table are for the rising period (R), the flat topping period (F), and the sum of the two (T = R + F). They are based on a pulse duration of four seconds, assuming 24-hour operation throughout the whole year or a total of 7.8896×10^6 pulses per year.

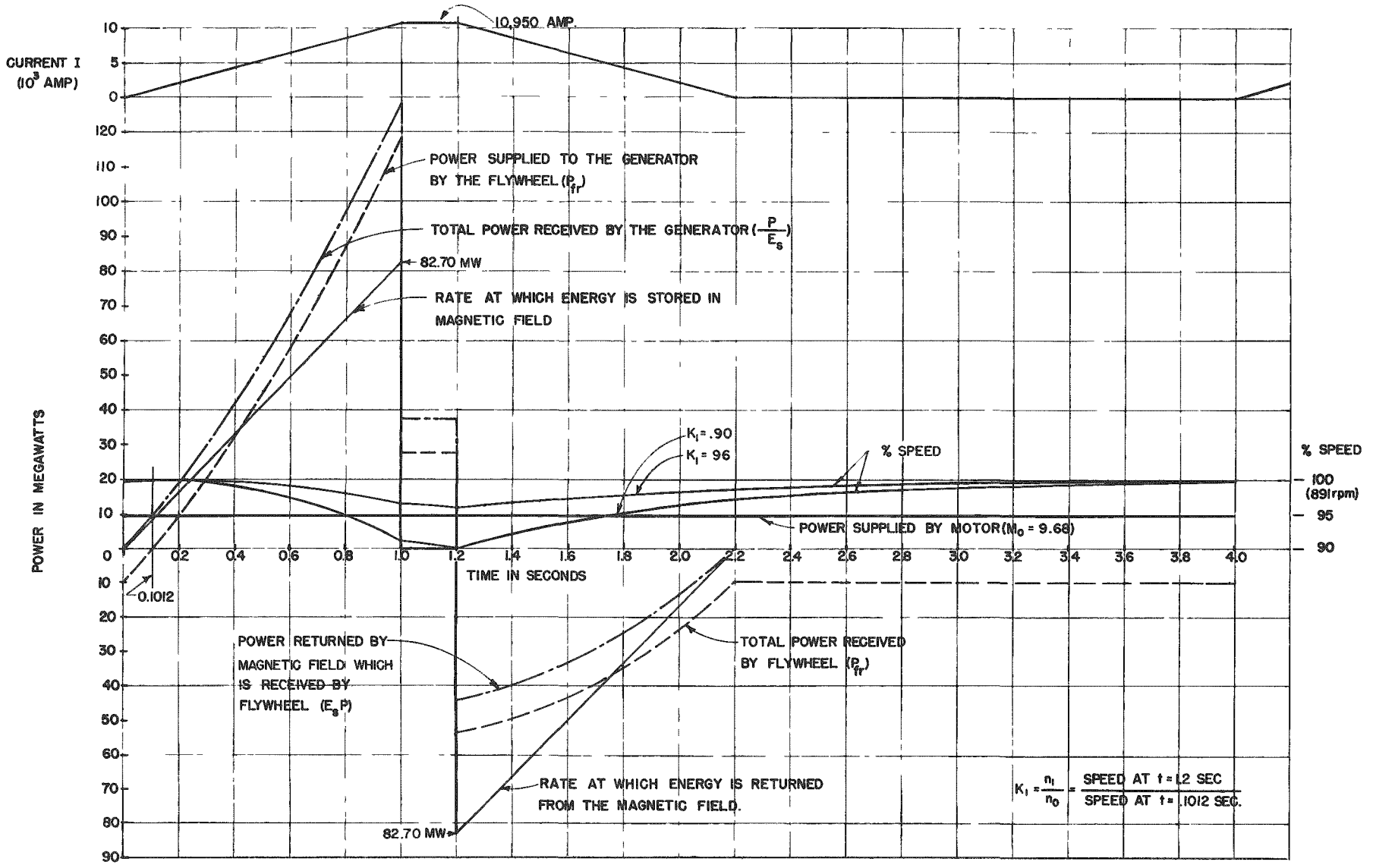

Fig. 4

Calculations on 704F

Table IV

SUMMARY OF RECTIFIER ARC-BACK EXPECTANCIES

Expectancies of Arc-back per Year per Tube

Magnet		Δt, sec	Case III							
			Nr = 144				Nr = 192			
Voltage, volts	Current, amperes		n = 5			n = 7	n = 5			n = 7
			R_5	F_5	T_5	T_7	R_5	F_5	T_5	T_7
10600	10950	0.2	14.8	127.6	143	0.10	3.6	31.6	35	0.014
	10948	0.24	12.4	151.9	164	0.12	3.0	37.7	41	0.017
	10007	0.35	9.3	185.5	195	0.14	2.2	46.0	48	0.019
	9017	0.55	6.1	233.0	239	0.16	1.5	57.7	59	0.022
	8273	0.76	4.1	275.6	280	0.17	1.0	68.1	69	0.024
	7647	1.00	2.8	315.7	319	0.18	0.7	77.9	81	0.026
	7091	1.30	1.9	354.8	357	0.20	0.5	87.5	88	0.027
	6587	1.58	1.3	394.2	396	0.21	0.3	97.0	97	0.029
10600	6118	1.93	0.8	434.9	436	0.22	0.2	107.0	107	0.031
			Case IV							
12089	10950	0.20	17.5	341.4	359	0.407	4.3	85.6	90	0.57
11684	9450	0.39	9.2	382.3	392	0.36	2.2	95.3	98	0.51
11428	8500	0.59	5.5	406.2	412	0.33	1.3	100.9	102	0.46
11226	7750	0.82	3.4	419.8	423	0.20	0.8	104.0	105	0.42
11070	7175	1.06	2.2	431.3	433	0.28	0.5	106.6	107	0.39
10928	6650	1.35	1.4	438.4	440	0.26	0.3	108.2	108	0.36
10800	6175	1.67	0.9	443.7	445	0.24	0.2	109.4	110	0.33
10672	5700	2.07	0.5	446.6	447	0.22	0.1	109.9	110	0.31

R_5 = rising period (n = 5)

F_5 = flat-topping period (n = 5)

T_5 = (R_5 + F_5) period (n = 5)

T_7 = (R_7 + F_7) period (n = 7)

The numbers n = 5 and n = 7 refer to the quality of the rectifiers. On the basis of published information, n = 5 should represent the worst that may be expected during the initial aging period of operation; n = 12 should represent the condition that may be approached after the aging period is completed; n = 7 represents a condition intermediate between the above two extremes.

It is assumed that each pulse lasts 4 seconds and that the accelerator operates 24 hours/day every day of the year.

Our current plan is to operate the accelerator with no flat topping for approximately one year. From the Summary Table (page 13) it is seen that during this period with 144 rectifiers the expectancy during the rising period with a maximum current of 10950 amp would result, under the worst condition (n = 5), in about 15 arc-backs per year per tube. Taking as an objective operation that corresponding to one arc-back per year per tube, this would mean that during the initial stage of operation with no flat topping we would have to limit operation to a maximum current of about 6400 amperes (approximately 16.0 kgauss, 9.3 Bev). It will be noted also that with the above objective of one arc-back per year per tube the use of 192 tubes would raise this initial current from 6400 to about 8300 amperes (about 20 kgauss, 11.5 Bev).

In addition, Table I, page 25 of PAD Summary Report ANL-6032 shows that when operating at 10950 amperes with 0.2 flat topping, each one of the 144 rectifiers is loaded to 57.10% of the manufacturer-assigned rating. This figure compares with 62.5 to 71% for the Cosmotron with no flat topping.

III. ZGS ELECTRIC POWER DISTRIBUTION

K. Burba

A 13.2-kv primary distribution voltage and 2.3-kv and 440-v utilization voltages have been selected for the ZGS. The 138-kv utility source and the complexity of the system imposed high interrupting capacities on the equipment. The system will be a resistance-grounded wye on the 13.2 and 2.3-kv sides and a solid-grounded wye on the 440-v side.

A primary selective system has been adopted for the primary distribution. Synthetic rubber-insulated, interlocked galvanized steel armored cables were specified: shielded 15 kv for the 13.2-kv system, nonshielded 5 kv for the 2.3-kv system, and 600 v for the 400-v distribution.

The following major equipment of the distribution system is currently under procurement:

1. The first of the two main power transformers: 18,750/25,000/31,250 kva, with forced air and oil cooling in two stages, 132-12.5 kv with ± 10% automatic tap changer under load on the low voltage side in increments of $\frac{5}{8}$%;
2. Thirteen unit substations with a total of 16,050-kva capacity and provisions for future increase by fan cooling on the indoor dry-type transformers, drawout-type air circuit breakers with an interrupting capacity of 60,000 amp rms at 480 v for the main breakers have been specified:
3. 2.4-kv switchgear comprising a total of two main air circuit breaker units and five large motor-starter units;
4. Twenty-one motor-control centers for the 440-v loads, with a total of 19 main and 240 branch circuit breakers all having a minimum interrupting capacity of 25,000 amp rms at 480 v.

IV. SEVEN-MEGAWATT (PEAK) POWER SUPPLY

K. Burba

A unique experimental power supply has been discussed, specified, and is now on order. It will be used initially in the ZGS Shop and Assembly Building to test all ZGS ring magnet blocks at full power.

The power supply will consist of the following major parts:

1. An outdoor 13.2-kv, primary switchgear with a 500-Mva interrupting capacity air circuit breaker;
2. An outdoor 12-phase rectifier transformer with a series autotransformer for fixed voltage taps and three interphase transformers, all in one tank insulated and cooled by a nonflammable liquid, rated at 3,250 kva;
3. 12 mercury arc rectifier tubes, vacuum-pumped ignitrons in a quadruple zig-zag connection, rated at 3,000 kw at 1,000 v(dc);
4. Master control cubicle;
5. Shorting switch cubicle with protective equipment for the test magnet coil, including a fast-acting switch and tungsten alloy irradiated spark gaps.

This power supply will produce in the 22.74-ft long magnet block test coil current pulses identical to the pulses in the ZGS ring magnet coil. These pulses will be triangular in shape with a rise time of one second from 0 to 10,950 amp, a decay time of one second and a rest time of two seconds. The voltage drop will be from 700 v at no load to 583 v at peak load.

The peak power for stored energy and losses during the rise period will be in the order of 7 Mw. The stored energy of 2.24 Mw-sec in the magnet test coil will be dumped back into the supply line by inversion of the rectifiers at the end of each rise time.

A temporary overhead line will feed this power supply from the ZGS main power transformer until permanent cable routing facilities will be installed in the buildings now under design.

The same power supply will be available later for experimental work at its full continuous dc capacity of 2.8 Mw.

V. RING MAGNET VACUUM CHAMBER

W. B. Hanson, F. W. Markley

A. Inner Vacuum Chamber

1. "Convair" Epoxy Chamber

The epoxy chamber described in the last report (ANL-6032) has now been completely tested. Several defects were found, but were corrected without too much trouble. Welding of the end flanges had destroyed the epoxy bond at the end of the "H" joints, and the welds themselves had some porosity. There was a greater amount of air in the epoxy glass cloth lamination than was desired. The entire "H" strip joint was porous, and internal cleaning of the bonded stainless strips was not satisfactory. After correction of these defects, the chamber pumped down satisfactorily. (See J. Moenich's report of degassing and pumpdown measurements made on this chamber -- JSM-6.) In the final comparison of this chamber to the "Spacemetal" chamber, its greater eddy current effect, greater chances of losing structural strength through radiation degradation, and greater danger of structural failure through brittle fractures of the epoxy "H" strip joint, plus various construction difficulties, led us to select the "Spacemetal" type of chamber for the final system.

Certain valuable information in bonding techniques, such as vacuum bagging on a heated platen table and the use of AF-31 nitrile phenolic bonding film, are a result of this prototype program. We therefore feel that it has served a useful purpose.

2. All Metal Chamber

Some consideration was given to an all metal inner vacuum chamber composed of convolutions of stainless steel about 0.010 in. thick. The technique of construction would be similar to that for forming a rectangular-shaped bellows. From the standpoint of minimum outgassing, this chamber would have been desirable; however, the cost of fabrication appeared to be prohibitive. Therefore, no prototype was made and the investigation was dropped.

3. "Spacemetal" Chamber

The inner vacuum chamber which is to be used in the synchrotron will be constructed of "Spacemetal." This is a metal sandwich made up of two outer skins of 0.006-in. thick material with a 0.002-in. corrugated core metal in between. The total height of the sandwich is approximately $\frac{5}{32}$ inch. This material was developed by North American Aviation Company under an Air Force contract, and is now produced and is commercially available from North American.

The prototype work which has been done has utilized standard "Spacemetal," which is constructed of full-hard stainless steel. Because of its much superior magnetic characteristics and high electrical resistivity, the "Spacemetal" for the final chamber will be constructed of Inconel. Several samples of "Spacemetal" made from Inconel have been produced for us by North American, and magnetic tests with this material have been made and are still in process. Samples of "Spacemetal" have been inserted into the 1/7-scale straight dc magnet; the effect of hard stainless steel "Spacemetal" is 50 gauss at a full-scale field of 20,000 gauss. The effect of annealed Inconel under a similar condition is 1 gauss in 20,000. At low field, the effect of hard stainless steel "Spacemetal" is 9 gauss with a field intensity of 1,000 gauss, as compared to virtually zero effect from annealed Inconel. Tests using hardened Inconel and annealed stainless steel are still pending.

A 1/4-scale model using stainless steel "Spacemetal" has been fabricated for use in the 1/4-scale pulsed model magnet. This test is now in process and a similar model made from Inconel is now being constructed.

The general construction of the inner vacuum chamber is shown in Fig. 5. The top and bottom of the chamber are constructed of "Spacemetal" sections, $5\frac{3}{4}$ in. wide, each of which is insulated from its neighbors. The side walls are continuous for a length of ten feet on one side and continuous for the entire length of the chamber on the other side, for the purpose of discharging the electrostatic charge on the inside surface of the chamber. The purpose of the insulated joints is to reduce the effects of eddy currents on the magnetic field.

The internal core of the "Spacemetal," which is open to the rough vacuum side of the chamber, is filled with epoxy resin. The purpose of filling is threefold:

a. to reduce pumpdown time for the rough vacuum system;

b. to provide insurance against vacuum leaks which might possibly develop at some time during the life of the chamber; and

c. to increase the structural strength of the chamber by about 40%.

Two prototype chambers have been constructed to prove the feasibility of constructing the final chamber in this manner. The first chamber was three feet long and full scale in cross section. This chamber was laid up with no vacuum leaks and was tested by the Vacuum Group.

The results of these tests are described in another section of this report. The only major problem which occurred during the construction of the three-foot prototype was the fact that most of the bonded joints were electrically shorted.

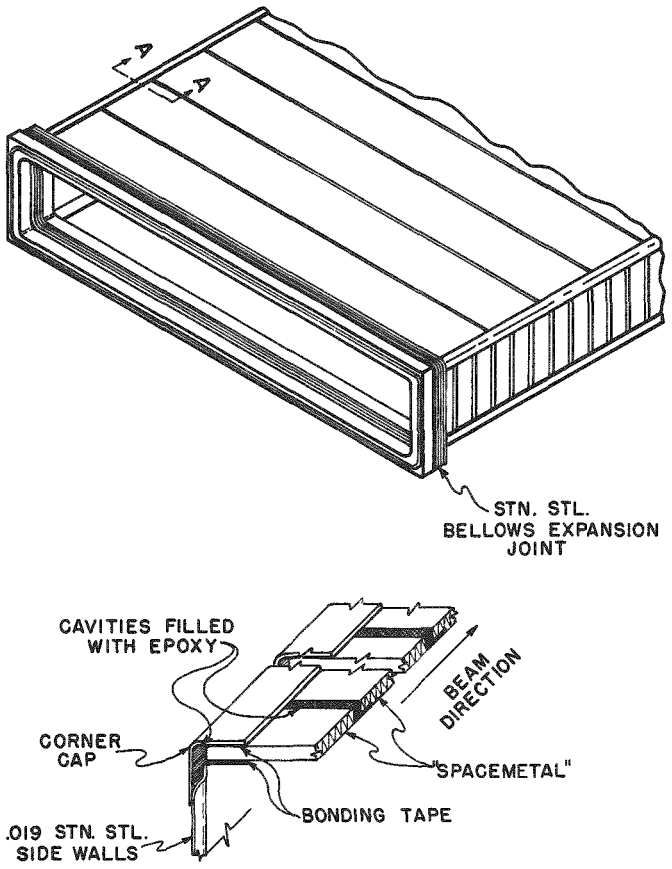

Fig. 5

Inner Vacuum Chamber

A twenty-five-foot chamber is now in the final stages of construction and was built chiefly for the purpose of making vacuum conductance and outgassing tests using a pumping system similar to that to be used on the final chamber. An investigation to study the problem of eliminating electrical shorts was carried on in conjunction with the construction of this chamber and the results are described in the section on "Bonding and Filling of 'Spacemetal.' "

The procedure for fabrication of the final chamber is to be as follows:

a. Cut "Spacemetal" into $5\frac{3}{4}$-in. sections.

b. Machine an overlapping lip on one side of each section.

c. Bond sections together on a hot platen table, using vacuum bag techniques, into sheets approximately 10 feet long. A template establishes the proper curvature for these ten-foot sections.

d. Joggle along one edge of the "Spacemetal" to provide a radiation shield to the bonded corner joints.

e. Vacuum test 10-foot sheets.

f. Bond top and bottom "Spacemetal" sheets to channeled side walls. Bonding pressure has been accomplished by clamping and curing in an oven. The use of a vacuum bag technique for this bonding operation is also being investigated.

g. The ten-foot sections are impregnated with epoxy resin, by means of a combined vacuum and pressure technique. The process involves placing the section on its edge and pulling a vacuum on the top edge while introducing epoxy under pressure along the lower edge. This technique was not used in the prototypes but is to be used in another five-foot section which is now under construction.

h. Join ten-foot sections of chamber together, using an internal hot platen fixture and applying clamping pressure from the outside.

i. Vacuum test the complete chamber, using an internal helium pressure of about 10 mm Hg.

j. Vacuum test, using an internal vacuum and a helium probe on the outside. This technique of vacuum testing is under investigation and involves the use of an internal rubber bag and a conductance grid between the outside of the bag and the inside of the vacuum chamber in the area being tested.

4. Bonding and Filling the "Spacemetal"

The Minnesota Mining and Manufacturing Company's nitrile phenolic bonding tape "Scotchweld AF-31" was selected for bonding the "Spacemetal" chamber because of its high bond strength, controlled flexibility, good peel strength and handy film form. The flow of this tape under

bonding temperatures and pressures is sufficient for good wet-out and is easier to clean up than an epoxy adhesive or other high-flow adhesive. The outgassing of this tape, reported elsewhere in this report, is greater than that of many epoxies, but it will still be quite satisfactory. The radiation degradation of this material is more rapid than many epoxies, according to information received from the Minnesota Mining and Manufacturing Company. However, its greater initial bond strength offsets this, so that its residual strength at about 1000-Megarad total dose is similar to that of epoxy. The overlap shear strength of the bond to stainless is limited by the yield strength of the thin stainless rather than by the adhesive or cohesive strength of the AF-31 bond. Tests on the bond strength to Inconel will be conducted soon. Because higher initial strengths may extend the radiation life, we will carefully etch and prime the metal before bonding, even though the former treatment is not necessary to produce a bond which initially is stronger than the steel. The etching is also believed to be necessary to insure consistently vacuum-tight bonds, and may prove useful in eliminating electrical shorts. The etching treatment used on stainless steel is given below, and it will also be tried out on Inconel soon, but the high nickel content of the Inconel may require a different etchant.

a. Degrease with trichloroethylene.

b. Treat for 19 minutes at 120°F in a solution of 35 ml saturated sodium dichromate in 1 liter of concentrated sulfuric acid.

c. Wash in running tap water.

d. Wash in hot distilled water.

e. Air dry before priming with Minnesota Mining and Manufacturing Company's EC-1459 primer. After priming, air dry for 30 minutes, and then oven dry at 250°F for another 30 minutes.

An attempt to decrease electrical shorting across the bonds by a slight precuring of the AF-31 tape to reduce its flow did not work, because of poor final bond wetting. Several other methods were also tried but did not appear to be very satisfactory. Therefore, we now plan to eliminate shorting by bonding and curing a layer of AF-31 tape on one side of each lap joint and then bonding with a second layer of AF-31. This method appears to work well, and we believe that the increased area of AF-31 exposed to the high vacuum will not increase the chamber gas load excessively. This will be checked with another test section, however.

The epoxy to be used in filling the "Spacemetal" has not yet been selected. This material should bond well to Inconel, have a reasonably good thermal shock resistance, a low viscosity, long pot life, a low vapor pressure, and preferably be room-temperature cured. Work to select an appropriate epoxy formulation has begun and it will be tested on the five-foot chamber which is under construction.

B. Outer Vacuum Chamber

The outer vacuum chamber is composed of the upper and lower magnet blocks forming the top and bottom walls and gasketed side planks forming the side walls. The magnet block laminations are made vacuum tight by the interlaminar bonding material used in the fabrication of the blocks. The individual blocks are to be vacuum tested after fabrication and sealed with epoxy resin from the outside if any leaks are detected.

Block-to-block sealing is to be accomplished by one of two methods. That of using a compressible rubber gasket between the blocks has been investigated and tested, and is described later. A second method of block-to-block sealing, which facilitates magnet assembly, involves the use of a polysulfide sealing compound, or equivalent, pumped into a groove which is milled into the face of each block. Figure 6 shows the shape of this groove. Tests using this technique are under way and are later described.

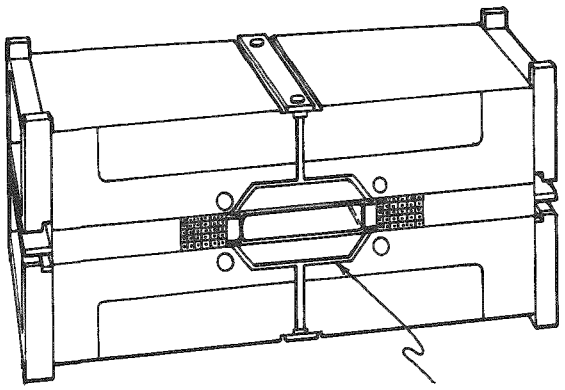

Fig. 6

Block-sealing Groove

All the blocks of the lower magnet pole will be assembled and sealed. A side-wall plank will then be bonded to the lower pole between the inside of the magnet coil and the outside of the inner vacuum chamber. Approximately $\frac{1}{2}$ x 2 in. will be provided between the side wall plank and the inner vacuum chamber for rough vacuum azimuthal conductance. The top of the side-wall plank will be grooved and gasketed to seal between the plank and the upper pole blocks. The upper pole blocks can be handled in pairs, so that half of the block-to-block seals can be made before final assembly. The upper blocks are then assembled, and there remain six joints per octant to seal by means of pumping sealing compound into the joints provided. The azimuthal gasket forms a "T" joint at the octant ends, thereby producing a seal between the rough vacuum chamber and the transition chamber.

The following test program for the outer vacuum chamber has been undertaken:

1. 1/4-scale Model Test

As described in the last report (ANL-6032), a gasket system for the rough vacuum chamber has been designed and tested on a 1/4-scale model. The tests were quite satisfactory. A flat rubber gasket, bonded in place with an epoxy polyamide adhesive, was used for the block-to-block seal. The side-wall seal consisted of Fiberglas-epoxy laminates bonded to rubber strips, which were in turn bonded to the pole faces (see Fig. 4, page 17, of Summary Report ANL-6032). However, a modified method of sealing is now being checked, as described in part 3 below. This method will be more convenient from an assembly point of view.

2. Full-scale Magnet Prototype Program

A full-scale magnet block has been constructed in order to check out the magnet lamination procedure described in the last report (ANL-6032). The results were quite satisfactory and only minor changes in the layup procedure were found to be necessary in the scale up from 1/4 to full scale.

3. Block-to-block Sealing Using Sealing Compound

Two tests are under way to determine the proper material and technique of pumping sealing compound into the grooves provided between the blocks. One test fixture has been made to full-scale joint dimensions. A polysulfide sealant has been pumped into the grooves to seal off the blocks and to form a seal between the upper and lower blocks and the azimuthal gasket. This test setup has been maintained at a continuous vacuum of approximately 15 microns for more than 1000 hours. Two small leaks have developed in the azimuthal gasket but no leaks in the block-to-block groove seal. The fixture provides for changing the joint thickness which will simulate expansion and contraction of the magnet due to temperature changes. Varying the gap width in steps of 0.002 in. will be the next phase of this program.

Another test fixture to determine the proper viscosity of sealant and to develop a technique of breaking the sealed joint between blocks when necessary is also under way. Lucite plates are being used for this test to facilitate viewing of results. The test indicates so far that it is feasible to seal this joint from the outside of the magnet with sufficient control of the flow of sealant.

C. Transition Chamber

Construction of a prototype transition chamber, shown in Fig. 3, page 15, of ANL-6032 , has begun and should be completed in June, 1960. The chamber will be constructed of epoxy-Fiberglas and lined with stainless

steel. It will be manufactured as a one-piece unit for maximum strength and vacuum integrity. The chamber will be produced in a closed, vacuum-tight mold, as follows:

1. The mold will consist of cured epoxy cores to form the inner cavities, and an outer steel box. These materials were chosen to give good release of all mold parts from the completed chamber through differential thermal contraction.
2. The assembled core will be tightly wrapped with style 143 glass cloth, Volan A treated. The direction of high strength will be the radial direction.
3. The steel outer mold will be assembled over the wrapped core, bolted in place, and vacuum sealed with RTV silicon rubber.
4. The mold will then be evacuated from the top and heated to 80°C, for a minimum of 16 hours.
5. Epoxy resin, degassed Epon 828 with 3 phr of boron trifluoride monoethylamine, will then be admitted to the bottom of the mold.
6. The mold will be allowed to fill, and then epoxy resin will be drawn through it until the emerging resin is seen to be bubble free.
7. The mold will then be let up to atmospheric pressure and cured. It is anticipated that no machining other than drilling bolt holes and vacuum piping holes will be necessary.

This work on the transition chamber, and all other plastics and adhesives work described in this report, has been the partial responsibility of R. D. Roman.

VI. VACUUM CHARACTERISTICS

J. S. Moenich

Inner Vacuum Chamber

The decision to use inner and outer vacuum chambers with a differential pumping system on the ZGS machine resulted in the fabrication and testing of three types of inner chambers. Some comparative data and the sources to more detailed information on the testing of these chambers are contained in Table V.

Table V

COMPARISON DATA

Test Chamber	Approximate initial pump down time (days)	Ultimate pressure achieved (mm Hg) (at equiv. pumping speed)		Approximate continuous gas load per 54-ft octant at room temp. ($\mu\ell$/sec)	
		Before Bakeout	After Bakeout	Before Bakeout	After Bakeout
Epoxy and Fiberglas-coated Vacuum Chamber*	15	1.7×10^{-6}	1.6×10^{-6}	3.15	2.9
Convair Chamber**	9	3×10^{-6}	4×10^{-7}	7.65	0.276
"Spacemetal" Chamber***	1	4.4×10^{-7}	2.6×10^{-7}	0.36	0.108

*Experimental epoxy Fiberglas-coated vacuum chamber JSM-5

**Vacuum tests-Convair inner vacuum chamber internal report to R. H. Lykken

***"Spacemetal" chamber - JSM-6

The performance of the "Spacemetal" chamber under vacuum exceeded that of the other two by a good margin. Ultimate and outgassing rates on the "Spacemetal" chamber, taken at room temperature and at the estimated 110°F operating temperature of the ring vacuum system, show very little change (see Fig. 7). This was not true with the Convair chamber, for instance. Its outgassing rate went up by a factor of three, even after a mild bakeout, when the temperature of the chamber was raised to 110°F.

A mild bakeout of the epoxy Fiberglas-coated vacuum chamber resulted in very little improvement in outgassing; but in the case of the Convair chamber it was especially helpful, and, in fact, reduced outgassing rate by almost a factor of thirty. The outgassing rate of the "Spacemetal" chamber, quite satisfactory before bakeout, was reduced by over a factor of three (see Fig. 7) after being subjected to the mild bakeout.

October 29 to December 22, 1959
Outgassing rate (Micron liters/sec)
"Spacemetal" chamber (3') at approximately 5 x 10^{-7} mm Hg.

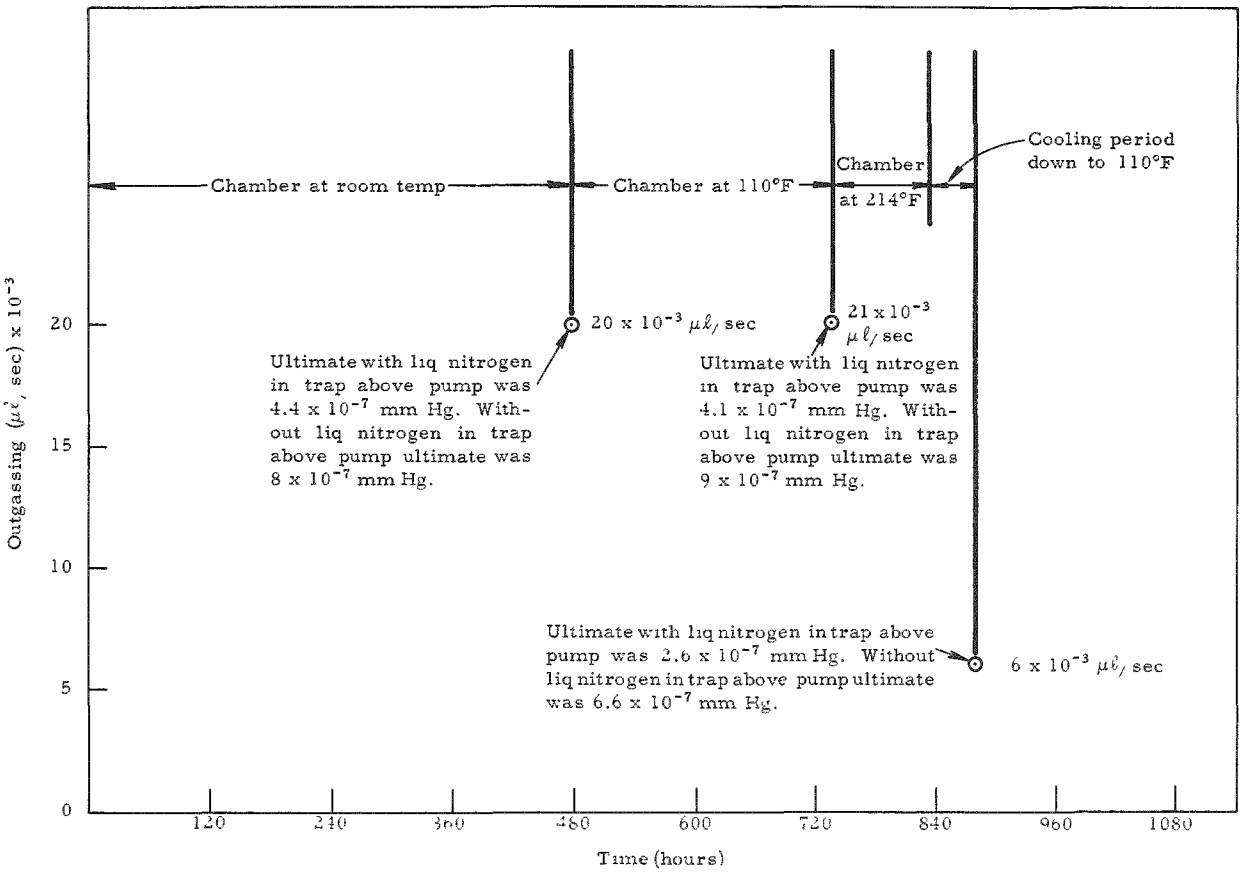

Fig. 7

Outgassing

Bakeout of the 54-ft section of the inner vacuum chamber required in each octant, especially under vacuum, would be difficult and quite expensive. The impractical nature of this problem necessarily points to the "Spacemetal" chamber as the only chamber, of the three tested, to be ideally suited to the impedance characteristics found in the vacuum envelope of the ZGS machine. Its low outgassing rates, even before bakeout, should result in a low ultimate pressure in the octant area and a reasonably small pressure gradient from the center of the octant to the pump.

Table VI is a chart indicating the pump-down time of the "Spacemetal" chamber under conditions listed thereon. Noteworthy is the difference in pump-down time to 1 x 10^{-6} mm Hg and 5 x 10^{-7} mm Hg with and without liquid nitrogen in the trap above the pump. Since this is the expected operating range of pressure in the vacuum system, it is apparent

Table VI

PUMP-DOWN TIME
"Spacemetal" Chamber

	Pressure mm Hg	LIQUID NITROGEN IN TRAP ABOVE PUMP				
		Chamber brought up from ultimate to atmospheric pressure with room air and left exposed to room air for:			Chamber brought up from ultimate to atmospheric pressure with dry nitrogen and left exposed to room air for:	
		2 hr	≈24 hr	2 weeks	2 hr	≈ 24 hr
		Time (hr)				
Chamber at room temp.	5×10^{-6}			0.75	0.60	
	3×10^{-6}			1.50	0.65	
	1×10^{-6}			15.00	0.90	
	5×10^{-7}			120.00	1.50	
Chamber at 114°F after bakeout at 214°F	5×10^{-6}	0.60	0.70		0.60	0.56
	3×10^{-6}	0.70	0.78		0.67	0.65
	1×10^{-6}	0.85	1.10		0.78	0.80
	5×10^{-7}	3.00	3.00		1.50	3.40
Chamber at 114°F after bakeout at 214°F No rate of rise curves during this series.	5×10^{-6}	0.22	0.23		0.20	0.28
	3×10^{-6}	0.32	0.37		0.27	0.40
	1×10^{-6}	1.00	1.70		0.70	1.40
	5×10^{-7}	3.40	7.50		1.70	7.00
		NO LIQUID NITROGEN IN TRAP ABOVE PUMP				
Chamber at room temp.	5×10^{-6}		0.65			0.35
	3×10^{-6}		2.00			0.90
	1×10^{-6}		100.00			35.00
Chamber at 105°F	5×10^{-6}	0.22	0.70		0.30	0.25
	3×10^{-6}	0.45	1.60		0.52	0.55
	1×10^{-6}	12.00	50.00		10.00	15.00
	5×10^{-7}	over 100	over 100		over 100	over 100
Chamber at 114°F after bakeout at 214°F	5×10^{-6}	0.30	0.32		0.26	0.34
	3×10^{-6}	0.65	0.95		0.40	0.65
	1×10^{-6}	8.50	12.00		7.00	11.00
	5×10^{-7}	65.00	60.00		over 100	over 100
Chamber at 114°F after bakeout at 214°F No rate of rise curves during this series.	5×10^{-6}	0.40	0.48		0.28	0.36
	3×10^{-6}	0.70	0.95		0.42	0.70
	1×10^{-6}	4.50	13.00			7.00
	5×10^{-7}	over 100	over 100			over 100

that valuable operating time can be gained by using low-temperature baffles or traps. Tests with the "Spacemetal" chamber indicate, however, that continuous low-temperature baffling during operation (-250°F or lower) may not be necessary and that rapid pump-down can be achieved by the use of retractable liquid nitrogen fingers that can be removed from the system after the first hour or two of pump-down. Experiments to further substantiate this possibility will be carried out during tests with the 25-ft inner vacuum chamber presently under construction.

VII. PLASTICS

F. W. Markley, R. D. Roman (Measurements by R. Vosecek)

A. Outgassing of AF-31 Nitrile-Phenolic Bonding Film

Since the last Summary Report (ANL-6032), we have confined our outgassing measurements to an investigation of the "Scotchweld AF-31" bonding film to be used in the construction of the "Spacemetal" inner high vacuum chamber. We have measured the outgassing rate of an unconditioned sample, and the effect on this rate of (1) high-temperature vacuum degassing, (2) exposure to room atmosphere for varying periods after previous degassing, and (3) exposure to dry nitrogen for varying periods after previous degassing. The results of these measurements are shown in Figure 8. Only linear approximations to the actual data are given in this figure.

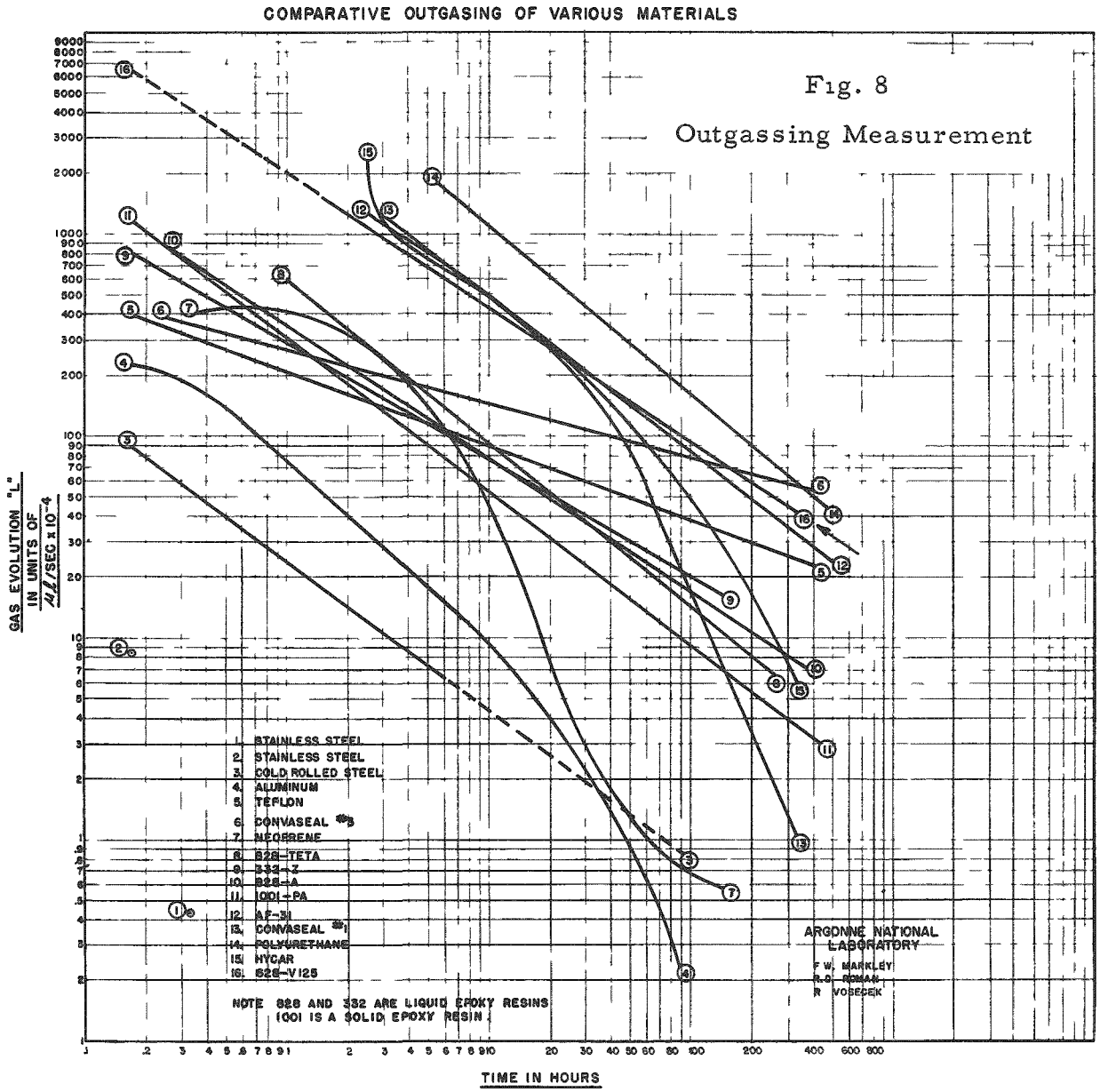

Fig. 8

Outgassing Measurement

The sample was prepared by curing several sheets of the film between Teflon-coated glass plates under a vacuum bag. A stack of alternate cured and uncured sheets was then cured in the same manner. A sample, 0.539 inch by 0.315 inch by 3.614 inches, was then machined from this stock with a clean, grease-free milling cutter. The diffusion of gases from the interior of this sample should be similar to the diffusion of gases from the $\frac{3}{8}$-in. wide thin film to be used in the "Spacemetal" chamber, since the latter is exposed to the vacuum on one edge only.

Curve No. 1 is the original pump-down of the unconditioned sample. At the end of this run, the sample was removed from the vacuum and exposed to the atmosphere for 16 hours. It was then returned to the vacuum system and run No. 2 was taken. At the conclusion of run No. 2, the sample was exposed to dry nitrogen at one atmosphere pressure for 16 hours. It was then returned to the vacuum system and run No. 3 was taken. After 350 hours, the sample temperature was raised from ambient to 300°F and kept there for 151 hours. The heat was then turned off and run No. 4 was taken as the sample was cooling down and afterwards. This high-temperature vacuum degassing is seen to lower the outgassing rate by two orders of magnitude. The slope of curve No. 4 would be even more steep if some unknown material coming out of the sample had not condensed on the cooler portions of the test chamber walls and subsequently been transferred to the surface of the sample as it was being moved to the clean test chamber. This material showed no visible tendency to diffuse out at ambient temperatures. However, the material that condensed on the chamber walls during high-temperature bakeout had a high enough vapor pressure at ambient temperatures to be slowly pumped out of the system.

At the conclusion of run No. 4, a series of exposures to dry nitrogen at one atmosphere pressure was begun. Each exposure was for a longer period of time than the previous ones. Curves 5, 6 and 7 were taken in this manner. At the conclusion of run No. 7, the sample was once again exposed to room atmosphere for 16.5 hours. Run No. 8 was then obtained The following conclusions are evident from the graph.

1. High-temperature vacuum degassing greatly reduces the outgassing. However, there will be such a small surface of AF-31 exposed to the vacuum on the "Spacemetal" chamber that such degassing should not be necessary (see J. Moenich's report on the vacuum testing of the 3-ft "Spacemetal" prototype chamber - JSM-6).

2. It will be very advantageous to let the vacuum system up to atmospheric pressure with dry nitrogen.

3. When evacuated AF-31 is let up to atmospheric pressure, the initial outgassing rate in subsequent evacuations depends on whether room air or dry nitrogen was used. The slope of the log outgassing versus log time curve, for short

atmospheric pressure exposures at least, depends on how far the sample was previously degassed and becomes steeper as the previous degassing was improved. Therefore, the chamber pump-down characteristics should always improve with time. No further vacuum outgassing measurements are contemplated in the immediate future.

B. The work on a ferrite bonding material of improved thermal conductivity mentioned in the last report (ANL-6032) has not been continued. The ferrite frames received have been considerably flatter than expected, so that we now expect to be able to handle the heat transfer problem by using a thin glue line of unfilled epoxy instead of a thick glue line of heavily filled epoxy.

VIII. THEORETICAL STUDIES

E. A. Crosbie, R. George, L. C. Teng

A. Analytical Studies of the $2\nu_y - \nu_x = 1$ Resonance (ANLAD-58)

The general Hamiltonian function for the motion of ions in the magnetic field of a circular accelerator was expanded in powers of x, y, and p_x, p_y. Beyond the second-order terms, only those terms contributing to the $2\nu_y - \nu_x = 1$ resonance were kept. A first-order perturbation calculation was made with these terms as the perturbation. In this manner, a general result giving the time behavior of the x and y amplitudes of betatron oscillations caused by this resonance in terms of first harmonic errors in the magnetic field, was obtained. When applied to the ZGS with $\nu_x = 3/4$ and $\nu_y = 7/8$, numerical calculations showed that even with 100 times the estimated field error the effect of the resonance is only barely noticeable during the 200 turns of injection time. This was checked out qualitatively by the computing machine result reported before. It is now considered definitive that the $2\nu_y - \nu_x = 1$ resonance will do no harm in the ZGS whatsoever.

B. Design Parameters for the DC Magnets of the ZGS, Assuming Infinitely Hard Magnetic Field Edges

Under the assumption of infinitely hard magnetic field edges for all the magnets, the properties of the trajectories of protons in the ZGS may be obtained by matrix calculations analytically. This method was employed to derive the design parameters of the DC magnets. The parameters of the DC magnets are adjusted so that:

(a) The central equilibrium orbit at injection follows the center line of the guide magnet.

(b) $\nu_x = 3/4$, $\nu_y = 7/8$ for the outer (15 in. from center line) equilibrium orbit.

(c) ν_x and ν_y stay within the limits for missing the inflector lip for 8 turns set in ANLAD-50 for any equilibrium orbit in the vacuum chamber at injection.

(d) The edges of the DC and the guide magnets are parallel.

The parameters are

Half turning angle $\phi_3 = 0.035000$

Half-length $s_3 = 1.66084$

Magnetic field $B_3(x) = \dfrac{715.76}{1 + 0.11840x + 0.0034765x^2}$ gauss,

where x is the radial distance from the center line. These parameters will serve as a starting point for more detailed computing machine calculations with the softness of the magnetic field edges taken into account.

C. Computing Machine Studies of Proton Orbits in ZGS Leading to Design Parameters of the DC Magnets with Soft Magnetic Field Edges.

The entire code, which requires about 180 minutes on "George" to integrate the orbit once around the accelerator, has been debugged, and checked and double-checked for given momentum and equivalent radius of a proton (and with assumed softnesses of the magnetic field edges). The procedure is, first, to find the equilibrium orbit by interpolation. Then, to get ν_x and ν_y for small oscillations, we only have to integrate two slightly off-equilibrium orbits across half of a symmetric sector (1 guide magnet and half of a DC magnet). The behaviors of orbits with large betatron oscillations can only be obtained by computing for the entire orbits throughout. The parameters of the DC magnets with soft edges are adjusted to perform as specified in (B). Preliminary results show that the DC magnets could be made shorter than those specified from study (B).

D. Study of the Matching Between the Linac and the Synchrotron

The matching of the phase-space areas of the beam exit from the Linac going through the focusing quadrupole magnets, the achromatic bending magnets and the inflector magnet, onto those required for the optimum injection into ZGS was studied before by J. R. Hiskes (JRH-2). However, that calculation was rather crude and no attempt was made to optimize all the available parameters of the coupling (or focusing) quadrupole magnets for precise matching. This has now been done in both the x and the y planes (assuming the beam to be going in the z direction). This leads to a system of equations (transcendental) giving the totally optimized parameters in terms of the precise matching. The solution of these equations will determine the design of the coupling quadrupole magnets.

E. Program for Calculating Parameters of a Pair of Quadrupole Magnets to Give Desired Matching

The system of transcendental equations arising from the study made above was solved numerically by coding it for the "George" computing machine. The Newton-Raphson method of approximation is employed and the program is ready for production problems.

F. Asymmetric Achromatic Bending Magnet Systems

Because of the interest of other accelerator construction groups, the calculation presented in ANLAD-48 was extended. In ANLAD-48 and for application to injection for ZGS, only symmetric achromatic bending magnet systems were considered, where a midpoint of mirror symmetry exists such that the halves of the magnet system up and down-stream from the midpoint are just mirror reflections of each other. Asymmetric achromatic bending magnet systems to guide a beam at a given spatial location and direction to another given spatial location and direction were studied. The system of transcendental equations giving the parameters of the magnets in terms of the mean momentum and the specified spatial locations and directions were derived. These transcendental equations can only be solved numerically.

G. Computing Machine Program for Solving Equations in Designing Asymmetric Achromatic Bending Magnet Systems

A program was written for "George" to solve the transcendental equations arising from the design of asymmetric achromatic bending magnet systems by the Newton-Raphson method. The program is finished, debugged, and ready for production problems.

H. Transverse Space-Charge Effects (ANLAD-59)

A closer look and a more detailed and more exact calculation were made for the transverse defocusing effect due to space-charge in a circular magnetic accelerator. The proper elliptical cross section of the beam was taken into account. The resulting formula when applied to ZGS gives 2×10^{13} to 7×10^{13} protons/pulse as the space-charge limit depending on which resonance line is fatal, and on the distribution of the protons around the ring. The possibility and procedure of neutralizing the space-charge effects by introducing free electrons into the beam in order to get beam intensities higher than 10^{14} protons/pulse were also studied quantitatively. Other difficulties associated with the attainment of very high beam intensities were discussed.

I. Lagrangian Formulation of the Motion of a Charged Particle in an Electromagnetic Field

The Lagrangian function for the motion of a charged particle in a magnetic field can be given either with time as the independent variable (time Lagrangian) or with the orbit length as the independent variable (space Lagrangian). In a general electromagnetic field the time Lagrangian is well-known. Here, we studied the procedure and formula for the transformation between space and time Lagrangian functions and

applied the procedure to derive the space Lagrangian in the case of general electromagnetic field and to discuss in detail the form, the condition for validity, and the applicability of both the time and the space Lagrangians and the Euler-Lagrangian equations obtained from them.

J. Hamiltonian Formulation of the Motion of Ions in a Sectorial Cyclotron or Synchrotron

The betatron and the synchrotron (phase) oscillations of ions in a sectorial cyclotron or synchrotron so far have been studied more or less independently. We have tried to derive these oscillations jointly, starting from first principles and proceeding purely according to rigorous mathematical rules. This way enables one to see better the relationship and the coupling between the two oscillations, the approximation made in decoupling the two, and the canonical natures of these oscillations.

We start with the general Hamiltonian function for the motion of a charged particle in an electromagnetic field present in a sectorial cyclotron or synchrotron (having a median plane and an N-fold rotational symmetry in that plane) with time t as the independent coordinate and the orbit coordinates [non-orthogonal coordinates $R = 1/2\pi$ (length of equilibrium orbit), $\theta = 1/R$ (length along equilibrium orbit), z = coordinate perpendicular to median plane] and their conjugate momentum variables as the dependent variables. We then transform to θ as the independent variable. Making the approximation of neglecting the electric field (assumed to be small), we can decouple the canonical equations in R and θ, and those in t. The equations in R and θ are immediately derivable from a reduced Hamiltonian function which can be expanded about an equilibrium orbit of the form R = constant. The canonical equations of the expanded Hamiltonian function give the usual betatron oscillation equations expressed in orbit coordinates. The remaining canonical equations in t describing the phase oscillation cannot, in general, be derived from a reduced Hamiltonian function. But in certain specific cases a reduced Hamiltonian function for the synchrotron or phase oscillation can be constructed. This Hamiltonian function can, then, be expanded about the synchronous quantities. The familiar phase-oscillation equations emerge as the canonical equations of the expanded Hamiltonian function. This study of deriving all the properties of a sectorial cyclotron or synchrotron beam from first principles is essentially the exhibition of the entire orbit theory for circular magnetic resonant accelerators.

K. Radiofrequency Accelerating Voltage Self-tracking Studies

Investigations of certain specific arrangements of the RF self-tracking schemes were presented by Cyril H. M. Turner (CHMT-1 and 2). We have now undertaken a thorough search and investigation of all possible schemes. Starting from the Hamiltonian formulation of the phase oscillation

obtained from (J) above, we impose a most general type of self-tracking where the frequency, voltage of the RF, and their rates of change are controlled by the radial position of the beam and the relative phase between the beam and the RF; and their rates of change. In this manner we can study the merits of all different types of self-tracking schemes and arrive at an optimum design. For the analytical studies the equations governing the phase oscillation were linearized. The results and conclusions were then checked by computing machines coded to solve the nonlinear equations as they are.

L. Programs for Studying Radiofrequency Accelerating Voltage Self-tracking Schemes

Two different programs were written for this study. The first follows the behavior of a large number of particles with random initial conditions of phase and energy around the machine, evaluates suitable averages of their phases and energies, and uses this information to control the voltage and the frequency of the applied RF. This program, which was previously reported in ANL-5864, was rather slow and behaved erratically when inadequate numbers of particles were taken.

A simplified second program was written; this solves the difference equations for the bunch of particles with the averaging processes already performed. Thus, this program traces the phase oscillation of the bunch as though it were a single particle. During the averaging process, certain moments of the distribution of particles in the bunch occur in the equations. The time behaviors of these moments have to be approximated from analytical studies. Compared with the first program, the second one is very much faster but suffers from the inaccuracy of the approximation made in taking the analytical moments of the distribution. However, this approximation is quite good and is not expected to affect the result noticeably. This second program is, now, also in production.

M. Phase Spaces and Beam Qualities

There seemed to be some confusion among different people using the terminology "beam quality" and "phase space density," especially when not all the variables specifying the beam were taken into account. It was shown that two independent systems of quantities (the "specific" and the "integrated") can be defined in the case when some of the beam variables are not explicitly exhibited. Examples were given to illustrate these two sets of quantities. For injection calculations for ZGS the integrated quantities which are more closely related to the Poincaré Invariants and the Liouville Theorem alone are of interest.

N. Solutions of Systems of Linear Differential Equations with Slowly Varying Coefficients

Systems of linear differential equations with slowly varying coefficients occur very frequently in connection with studies of the behavior of ions in accelerators. A general straightforward iterative approximation method for solving such a system of equations was developed, patterned after the adiabatic approximation used in solving the Schrödinger equation in quantum mechanics. This method leads directly to a convenient explicit form for the solution as a power series of the time derivatives of the coefficients.

O. Program for Evaluating the Characteristic Exponent of the Mathieu Equation

The characteristic exponent ν of the Mathieu equation

$$\frac{d^2x}{d\theta^2} + (a + 2b \cos 2\theta)\, x = 0$$

is important in many calculations of the alternating gradient type of focusing effect. Existing tables give ν over a mesh of a and b values much too crude for our purposes. This equation was coded for "George" to be integrated by the Runge-Kutta method. The resulting values of ν will be presented in a table.

P. Program for Studying the Depolarization of a Polarized Proton Beam Going through the Linac

This was studied independently by A. Burger and D. Cohen [Rev. Sci. Inst. 30 1134 (1959)] both analytically and numerically. Various approximations were employed in their studies. A more straightforward program, which traces the trajectory of a proton by transfer matrices and evaluates the precession of the proton spin by direct Runge-Kutta integration of the Larmor equation, was written for "George." The results agree qualitatively with those given by Burger and Cohen.

Q. SIREN Interpretive Routine for "George"

SIREN, a stored interpretive routine, permits us to write programs for the GEORGE computing machine in a simple and easily learned problem-oriented language. This language is a compatible extension of the BELL language, used interpretively with IBM 650. Programs for BELL-650 may be run on SIREN-GEORGE with greater speed and larger available memory. SIREN programs may be written with symbolic names for certain orders and for storage addresses.

Interpretive operation is always slower than operation with the machine language code, but it is much easier to create and debug the interpretive code. A plan for speeding up the operation is being studied.

R. Programs for Coil Design Problems

Several programs were written for problems of coil design. One of these generates the various dimensions relative to points located on the surface of the individual conductors. These dimensions will be used for checking the bending of the tubes. Another program gives the dimensions between similar points on different tubes. This will be used for the alignment of the tube assemblies. It should be noted that this work was done for the prototype coil, but that by changing only one number, the central arc angle, the work on the full-scale coil will be accomplished.

IX. RADIOFREQUENCY SYSTEM

M. Benade, R. Daniels, C. Laverick, J. Martin, J. Simanton, C. Turner

The radiofrequency program to be used in accelerating the protons in the synchrotron orbit will be established from reading the magnetic guide field. This will be accomplished by integrating the signal from a loop of wire wound about the guide magnet. The integrator for this has been constructed, tested, and found to have adequate qualities. It has a stability of about 3 parts in 10^5 for periods of a few weeks. The loop about the guide magnet will have a few turns built into the vacuum chamber wall of one octant. The signal for unclamping the integrator will come from an electron resonance probe in the magnet end. This probe is in the advanced stages of development.

The principal part of the master oscillator frequency program will be accomplished by permeability tuning. The detailed trimming of the program will be accomplished through dielectric tuning. The master oscillator package and permeability tuning system should be ready for final test by June, 1960. The 21-diode ladder network for trimming the program is completed and tested, and appears to be satisfactory with a noise level and long-term stability of about 1 part in 10^3.

The device for measuring frequency modulation noise in the radiofrequency system is completed and has been tested on static systems. It is designed for measurements in the range of frequencies from 1 Mc/sec to 20 Mc/sec. It is capable of detecting frequency jitter as small as 2 or 3 cycles per second in this range. The recurrence rate of this jitter can have any value from about 1 kc/sec to 10 kc/sec.

The radiofrequency power amplifier has been used in testing the ferrite frames for the cavity at flux densities up to somewhat higher than those anticipated during synchrotron operation. The prototype design of the power amplifier is scheduled for completion in June, 1960. The problems of interstage coupling seem to be solved. One of the intermediate stages is being redesigned.

Twenty-six of the 34 ferrite frames have been received from Philips in Holland. Average permeability tests have been made on about half of the ferrite frames. When completed, this will permit arranging the frames into symmetrical batches. Extreme variations in average permeability in going from frame to frame have been found to be about ±4% at all biases up to 10 oersteds.

Because of the expectation that the magnetic guide field may at times have a rate of rise as much as 25 kilogauss per second, the peak voltage capacity of the cavity and power amplifier had to be raised. This has resulted in increasing the number of cavity gaps from two to three and the

anticipated quantity of ferrite from 20 frames to 30 frames. The shortage of available straight section space for the cavity has resulted in compressing this assembly so that the three radiofrequency cells are in one box. The output of the power amplifier is designed to be placed across the three gaps in series.

A 12-diode ladder network has been constructed for the purpose of producing the cavity bias program from the integrator output which represents the field in the guide magnet. It appears to be satisfactory, with a repeatability of several parts in 10^4 and an accuracy of fit better than 1%. Under design at the present time is a device which will read the out-of-tune of the cavity and automatically trim the cavity bias for tuning closer than 1%.

Use will be made of beam induction electrodes for reading the radial position of the beam (R_1), the radial width of the beam (R_2), the vertical position of the beam (Z_1), the charge in the beam averaged over a few microseconds (Q), and the instantaneous charge at a certain position in the orbit averaged over a few millimicroseconds (q). One assembly of electrodes is expected to yield information about R_1, Z_1, and Q. A model of this set has been made and tested at low frequencies with a small wire. Partial tests have been made with a 1-Mev proton beam. A test assembly is under design which will use a pulsed electron beam and which will be used to test all of these electrode systems at particle velocity and bunch lengths encountered in the synchrotron. The R_1 system will be used to trim the master oscillator frequency to a preset orbit radius by supplying a correction signal to the dielectric-tuned portion of this oscillator. This control loop is intended to be fast enough to iron out coherent synchrotron oscillations and to reduce beam wobble due to guide magnet ripple. The q system will be used to observe the charge distribution within a single orbit turn and a single bunch of protons. It will also be used to read the phase angle between the cavity voltage and bunches of protons. Provision will be made to inject a fast correction signal from this phase detector into the dielectric-tuned portion of the master oscillator. The R_1 and q feedback loops probably will be separated by band pass filters. Both of these beam-tracking loops can be offset for programming the beam into targets. The R_2 system will be used for observing the damping of the radial beam oscillations and buildup of noise in the beam.

X. INJECTION SYSTEM

M. Abdelaziz, R. Castor, D. Cohen, P. Livdahl, J. Mech, W. Myers, R. Perry, A. Yokosawa

A. 800-kv Power Supply

A purchase contract has been awarded to Emile Haefely and Company of Basel, Switzerland, for an 800-kv cascade power supply for the preaccelerator. This system includes all equipment necessary for maintaining the dc output voltage constant to ±0.1% with a pulsed ion beam of 200 ma. Delivery is expected in December, 1960.

B. Present Status of Ion Sources Testing and Beam Acceleration

The pyrex ion source of F. Schneider has been tested for different sizes of the extraction canal. So far the source has been shown to be capable of developing a beam current of at least 70 ma. The beam was accelerated up to 220 kv through the accelerating column.[1] The results seem to indicate that none of the beam was lost during the acceleration. The test will be continued to study stability and long life of the source. The proton percentage of the beam will be measured by an analyzing magnet which is under construction.

As indicated by Schneider, the special shape of the ceramic cup was introduced to prevent the secondary emission from cathode. An attempt will be made to improve this situation further by changing the shape of the cup and material of the cathode.

The Duoplasmatron ion source was purchased from the High Voltage Engineering Corporation, Burlington, Massachusetts. The power supply, high-voltage insulation, and vacuum supply for this source are completed. The testing is being performed.

C. Trajectories of Nonparaxial Rays (AY-MS-1)

The dynamics of protons in a cylindrical three-electrode Einzel lens system has been investigated, taking into account the space charge. The differential equation governing the proton path was derived and is

$$\frac{d^2r}{dz^2} = \frac{1 + \left(\frac{dr}{dz}\right)^2}{2V}\left[\frac{\partial V}{\partial r} - \frac{dr}{dz}\frac{\partial V}{\partial z} + \frac{I}{2\sqrt{2}\,\pi\left(\frac{e}{m}\right)^{1/2} V^{1/2} r}\right]$$

in MKS units.

---

[1] Fechter and Saulys, ANLAD-53.

The value of the radius and slope of the marginal and inside rays of the beam were computed. It was concluded that the geometry of electrodes used in this calculation is not adequate for higher values of beam current because of the aberration effect. More complete analysis for the general case is being prepared. The emittance figure at various points will be calculated in terms of the geometry of electrodes, applied voltage, and beam current.

D. Beam Quality Measurement

A measuring device for the beam quality has been studied. The emittance of the beam at 50 to 300 kev will be obtained from x, θ_x or y, θ_y curves, where x and y are measured from the center of the beam. Two slits of small opening at certain intervals are being prepared. The first slit defines the value of x or y and the angle of divergence is determined by adjusting the second slit, which is followed by the Faraday cup. The density distribution in the phase space will also be measured.

E. Duoplasmatron Ion Source (AY-1 and AY-2)

The formation of the plasma boundary with respect to the applied extraction potential is being studied with the help of the electrolytic tank. It is aimed at establishing conditions for forming an ion emission surface which is optically favorable.

Recently a powerful ion source, a modified duoplasmatron ion source, was introduced by Frohlich.[2] Based on his results, further study will be made on the following aspects:

1. Effect of cathode space and location of filament with respect to the beam current.
2. Effect of canal-anode distance to the proton percentage.
3. Function of the intermediate electrode potential.
4. Seek for higher values of the arc current.

It is hoped to obtain higher values of the beam current and better proton percentage than the original duoplasmatron ion source. The beam quality is expected to remain the same.

F. A Study of Extraction System of CERN RF Ion Source (AY-3)

Equipotential lines between an assumed plasma boundary and cathode were studied by an electrolytic tank. Most of the potential lines seem to be parallel to each other except in the vicinity of the plasma boundary. One can start the perveance calculation by assuming plane-electrode space-charge flow.

---

[2]H. Frohlich, Nukleonik, Band 1, Heft 5 (1959).

For a given perveance, the proton trajectory in the canal will be calculated. The length of the canal will be determined to satisfy the most favorable ion optics by shortening the drifting region.

G. Accelerating Column

The results of tests which have been made so far on the 300-kv high-gradient accelerating column[1] have given us greater confidence in the ability of this column to control a high-current ion beam against space-charge blow-up. Results are not yet conclusive, but are sufficiently encouraging that plans for incorporating this feature into the preaccelerator column are being drawn up. In addition to a 300-kv high-gradient section (40 kv/in. external and 160 kv/in. internal) immediately following the ion source, the column would have a 450-kv low-gradient (10 kv/in. external) section, with the possibility of pushing the ground electrode a considerable distance into the column to increase the gradient inside this section by effectively reducing its length in vacuum.[3] The overall design of the column is such that the high-gradient section could be replaced by a low-gradient section. The entire column could then become more conventional in design without other modifications.

H. Service Platform

A lift platform has been designed which will make all parts of the 800-kv power system and the accelerating column accessible for assembly and servicing. A minimum of time delay in servicing the unit and a maximum of personnel safety were the basic criteria in the design.

I. Linac Radiofrequency System

The setting up of the linac radiofrequency system at Continental Electronics Manufacturing Company's Dallas, Texas, plant, although somewhat behind the schedule originally reported in ANL-6032, is proceeding satisfactorily. It now appears that operational tests will commence during the month of April on such units as the hard-tube modulator, the 50-kv high-voltage rectifier, and the 32-μ f storage capacitor.

Preliminary testing of other major units has been limited to bench checks intended to confirm design criteria. Units in this category include the radiofrequency exciter, the intermediate power amplifier, the pulse generator and synchronizer, the fault amplifier and crowbar, and the pulse driver.

The filament rectifier for the A2346F has been tested to full output; the water distribution unit and the ac distribution unit are completely assembled and installed at the test site. Wiring of the control console is nearing completion as is much of the inter-unit wiring at the test site.

[3] This feature was first proposed by L. Hobbis (private communication).

Bench tests have been conducted on the radiofrequency exciter, which indicate that it conforms to the stability and tuning range requirements. The intermediate power amplifier has been operated through its final (RCA 7213) stage for which only the cavity design remains to be debugged. No actual construction has been completed for the 4W20,000 driver or for the A2346F final amplifier stage, although the design is progressing satisfactorily.

All of the transmitter components are to be installed in a compound approximately 70 feet long by 10 feet deep by 8 feet high. All instrumentation can be accomplished outside the confines of this enclosure. Control and interlocking will permit completely automatic startup and shutdown of the transmitter from either a local or remote "start" - "stop" button. In the event of any of a number of faults, transmitter shutdown is likewise automatic.

It now appears feasible to drive the waveguide directly from the output cavity of the A2346F without any intermediate transmission lines. This makes it possible to drive the linac tank from below with a waveguide approximately $2\lambda_g$ long, located near floor level. Thus it will be possible to minimize the number of adjustable tuning stubs required to match the final amplifier to the load.

J. Linac Tank

A purchase contract for fabrication of the linac tank sections has been awarded to Lukens Steel Company, Coatsville, Pennsylvania. Lukens has subcontracted the machining on the tank to Cleveland Diesel Corporation. Work on the tank is now in progress, with delivery of all sections scheduled before March 31, 1961.

K. Drift Tubes

Machining work on the prototype drift tubes has been completed and final assembly of one of these with quadrupole magnet installed is complete. The end cap is soldered to the body using a 95%-5% tin-silver alloy which melts at 200°C. No damage to insulation on the magnet coils is observed after heating to this temperature, and vacuum-tight joints are easy to achieve.

Work on final drift tubes is now under way and a production schedule is being set up to meet delivery requirements.

L. Linac Quadrupole Magnets

Four prototype magnets have been built and tested for field gradient and power requirement, and all approximate the computed values

in this respect. The harmonic content of the field has been determined for two of the magnets at a radius of $\frac{1}{4}$ in. The sum of all harmonics above the second is found to be less than 1% of the second.

Because of the difficulty encountered in finding a satisfactory high-silicon steel, the poles of the magnets for the linac will be made of Armco magnet iron; the yokes will be made from 1015 carbon steel. Aging of the steel will be accomplished by heating at 500°C for several hours after finish machining. Production of these magnets is now in progress. Coils will be potted in the magnets using an epoxy filled with calcium carbonate to reduce shrinkage.

M. Quadrupole Power Supplies

Specifications for linac quadrupole power supplies are now completed and ready for bid solicitation. These are to be solid state rectifier units with good regulation and low ripple.

N. Injector Vacuum System

During the last year developments in the use of gettering-type vacuum pumps have led to reconsideration of the type of pumps to be used for the injector system. Present plans call for use of nine gettering pumps on the linac cavity, together with one mercury diffusion pump with a low-temperature vapor trap (using either liquid nitrogen or a refrigeration system). With this combination, the diffusion pump can be used to reduce the cavity pressure during pump-down to the region where the gettering pumps start readily, and it will also prevent a possible buildup of argon pressure which could occur with certain types of gettering pumps. This arrangement greatly reduces the complexity and cost of the system compared with that using mercury pumps throughout.

Design of the system on the above basis is essentially complete and some of the components are on order, with all other major components to be placed on order very soon.

O. Cooling System

Prototype arrangements have been made for cooling system headers, valves, flow switches, etc., for both the linac drift tubes and the quadrupole magnet coils and busses. Many of the required components for the final system are ordered, and the assemblies will be so made that they can be mounted on the individual linac tank sections as soon as the latter are received from the fabricator. These headers will then be connected by flexible tubing to the main cooling headers after the tank sections are placed on their supports.

P. Building Design

Considerable time and effort have gone into checking with the architect-engineer on various features of the Injector Building design in order to insure that provision is made therein for all requirements of the Injector System, and that space interferences will be minimized.

Q. Production Testing of Linac Quadrupole Magnets

The machinery to production-test the 124 quadrupole magnets is in the final stages of assembly and debugging. Some time ago it was decided that care must be taken to insure that the magnetic centerline misalignments be less than 0.003 in., that the relative magnet gradient errors be less than 1.5%, and that the possibility of a magnet failure after some years of operation be very small. The testing machinery has been designed to deal with these three tests; each magnet will be checked both before and after enclosure in its drift tube.

The heart of the testing arrangement is a "long" search coil which rotates at about 3800 rpm, and which can be both translated and skewed with respect to the magnet or drift tube. The search coil signal, via slip-rings, is fed into an electronic system consisting of a harmonic analyzer, a voltmeter-filter network, etc. The search coil has been designed for good sensitivity to all field harmonics; the fundamental harmonic (3800 cpm) component is zero only when the coil rotational axis coincides with the quadrupole magnetic centerline.

The system is mechanically designed around a Bridgeport milling machine, which provides the rotating shaft, and has been altered to provide all degrees of freedom of the search coil with respect to the magnet or drift tube. Four reference numbers will be recorded for each encapsulated magnet; two numbers for the position of the magnetic centerline half-way down the magnet, and two numbers for the longitudinal and polar angles of this line. These numbers will be used as corrections during alignment of the drift tubes in the linac tank. Power losses, gradient calibration, and ruggedness will also be measured and dealt with during testing with the Bridgeport mill arrangement.

XI. RING MAGNET COIL

W. A. Siljander

The preliminary design stage of the ring magnet coil program has been concluded. The final design stage is under way.

The following design criteria have been established:

1. the magnetic, electrical and physical parameters;
2. the material specifications for the copper, insulation, adhesive, and mechanical securing devices;
3. the fabrication procedure including the curing and bending jigging design; and
4. the installation procedure

Items 2 and 3 have been determined by a vigorous research and development program at the National Electric Coil Division of McGraw Edison Company.

This program was initiated in the spring of 1958 and will be concluded on the completion of the 22-ft prototype coil now under fabrication. It is anticipated that this coil will be completed in the fall of 1960.

Full-scale test specimens of the final design have been fabricated and undergone mechanical and electrical tests at Battelle Memorial Institute and the National Electric Coil Division. The results of these tests indicate that the following electrical and mechanical strengths can be anticipated for the final ring magnet coil.

Electrical

1. Voltage breakdown to ground. 30-35 kv;
2. Voltage breakdown layer-to-layer greater than 10 kv;
3. Voltage breakdown turn-to-turn greater than 5 kv.

Mechanical

1. Ultimate tensile and compressive strengths of 34,300 psi;
2. Ultimate tensile and compressive strength dropped less than 4% after fatiguing over 45 million cycles;
3. Maximum deflection in tension remained constant during the fatiguing under loads of five times the design operating loads.

Figure 9 is a photograph of the full-scale coil cross section cut from a full-scale test specimen. It can be noted that an extremely accurate and symmetrical conductor stacking can be achieved if the following controls are exercised:

1. Careful control of the copper conductor drawing operation so that opposite sides are parallel to within 0.001 of an inch total, adjacent sides perpendicular to within ± 0°15', and all sections kept from twisting along the entire length to within ± 0°15'.
2. The selection of epoxy and glass laminate with controlled thicknesses to ± 0.002 of an inch for the turn and layer insulation.
3. A two-stage pressure cure process.

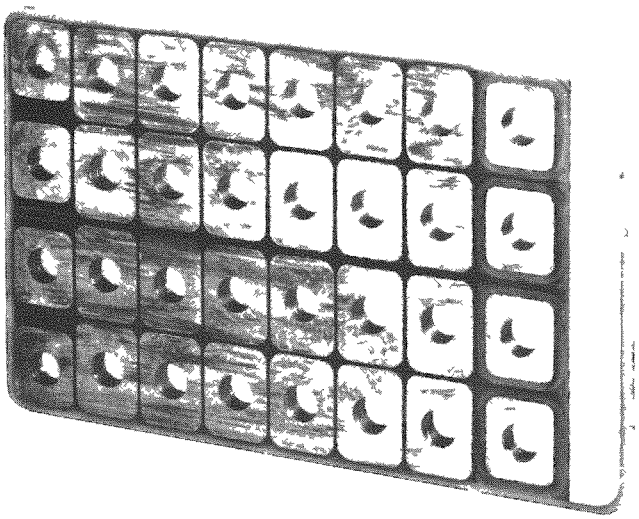

Fig. 9

Full-scale Coil Cross Section

In addition to the glass-based epoxy laminate for the turn and layer insulation, the combined ground insulation and outer mechanical wrap tying the whole section together will consist of multiple servings of epoxy-impregnated glass fiber tape, Minnesota Mining and Manufacturing Company's "Scotchply" crossply type, primarily for the ground and unidirectional for the outer wrap.

The establishment of the above-mentioned design criteria should enable the final design drawings, lists and specifications to be completed in the summer of 1960.

XII. AUXILIARY CALCULATIONS

D. Cohen, W. Myers

A. Required Beam Properties at the Inflector Exit

Some of Teng's work has been reviewed and calculations performed to see what variations and controls are necessary on the radial and vertical phase-space figures. Each figure inherently contains five independent parameters. It was felt that all ten parameters should be made independently variable within certain limits; this insures that the injector and matching system produce no serious limitation to synchrotron firing-up procedures and subsequent normal trimming operations.

B. Proton Depolarization in the Synchrotron

It is hoped that eventually the synchrotron will produce polarized protons; polarized sources are now being developed, and it has been shown that the polarization can be maintained during injection. Unfortunately, no reliable method has yet been found to calculate the amount of depolarization during synchrotron acceleration. Both computer tracing and a straightforward analytical harmonic treatment produce large errors. Perhaps some information may be obtained by an elaborate extension of Liouville's Theorem to a space including spin variables.

C. Fluorescent Screens

During the firing-up period of the synchrotron the beam position during injection will be determined largely by means of fluorescent screens viewed by television cameras. Calculations are in progress to find such parameters as optimum wire size and spacing in the screens, thickness of fluorescent layer, light intensity, etc.